RSC Advances

PAPER

View Article Online
View Journal | View Issue

Cite this: *RSC Adv.*, 2022, **12**, 12913

Design, synthesis, *in silico* docking, ADMET and anticancer evaluations of thiazolidine-2,4-diones bearing heterocyclic rings as dual VEGFR-2/EGFR^{T790M} tyrosine kinase inhibitors†

Nada A. A. M. Aziz,*[a] Riham F. George,[b] Khaled El-Adl*[ac] and Walaa R. Mahmoud*[b]

Fourteen recent thiazolidine-2,4-diones bearing furan and/or thiophene heterocyclic rings have been designed, synthesized and assessed for their anticancer activities against four human tumor cell lines HepG2, A549, MCF-7 and HCT-116 targeting both VEGFR-2 and EGFR tyrosine kinases. Molecular design was carried out to investigate the binding mode of the proposed compounds with VEGFR-2 and EGFR receptors. HepG2 was the most susceptible cell line to the influence of our derivatives. Compounds **5g** and **4g** revealed the highest activities against HepG2 (IC_{50} = 3.86 and 6.22 μM), A549 (IC_{50} = 7.55 and 12.92 μM), MCF-7 (IC_{50} = 10.65 and 10.66 μM) and HCT116 (IC_{50} = 9.04 and 11.17 μM) tumor cell lines. Sorafenib (IC_{50} = 4.00, 4.04, 5.58 and 5.05 μM) and elotinib (IC_{50} = 7.73, 5.49, 8.20 and 13.91 μM) were used as reference standards. Furthermore, the most active cytotoxic compounds **4d**, **4e**, **4f**, **4g**, **5d**, **5e**, **5f** and **5g** were selected to assess their VEGFR-2 inhibitory effects. Derivatives **5g**, **4g** and **4f** were observed to be the highest effective derivatives that inhibited VEGFR-2 at the submicromolar level (IC_{50} = 0.080, 0.083 and 0.095 μM respectively) in comparison to sorafenib (IC_{50} = 0.084 μM). As well, compounds **4d**, **4e**, **4f**, **4g**, **5d**, **5e**, **5f** and **5g** were additionally assessed for their inhibitory activities against mutant EGFR^{T790M}. Compounds **5g** and **4g** could interfere with the EGFR^{T790M} activity exhibiting stronger activities than elotinib with IC_{50} = 0.14 and 0.23 μM respectively. Finally, our derivatives **4g**, **5f** and **5g** showed a good *in silico* calculated ADMET profile. The obtained results showed that our compounds could be useful as a template for future design, optimization, adaptation and investigation to produce more potent and selective dual VEGFR-2/EGFR^{T790M} inhibitors with higher anticancer activity.

Received 19th February 2022
Accepted 22nd April 2022

DOI: 10.1039/d2ra01119k

rsc.li/rsc-advances

1. Introduction

The thiazolidine-2,4-diones (TZDs) as heterocyclic compounds have been disclosed to be a potential scaffold that play an important role in cancer therapy. TZDs were proved to exhibit anticancer activity in a wide variety of experimental cancer models by affecting the cell cycle, induction of cell differentiation and apoptosis as well as by inhibiting tumor angiogenesis.[1–3] Tumor angiogenesis is a fundamental marker for the growth and metastasis of malignant tumors.[4]

Lung cancer is the chief reason of cancer mortality, with nearly 85% of lung cancers being NSCLC. Since 2004, EGFR-sensitizing mutations have been established as driver oncogenes for NSCLC that predict response to EGFR tyrosine kinase inhibitors (TKIs).[5] EGFR mutations occur in 7% to 37% of NSCLC cases in white patients and 40% to 64% in Asian patients.[6] Regardless of ethnicity, these mutations more often present in women, nonsmokers, and those who have adenocarcinoma histologic diagnosis.[6] In approximately 90% of cases, EGFR-mutant NSCLC tumors harbor an exon 19 deletion or exon 21 L858R mutations, both of which render tumors sensitive to EGFR TKIs patients.[7] EGFRTKIs have been established as first-line therapy, in the metastatic setting, because of its progression-free survival (PFS) benefit and excellent tolerability.[5] Resistance to EGFR TKI therapy inevitably arises, even though initially effective and patients' progress. The 5 year survival rate for patients with EGFR-mutant metastatic lung cancer is around 15%.[8] Thus, the foundation of novel therapeutic strategies is necessary to improve patient outcomes. One aspiring complementary target of EGFR suppression in NSCLC

[a]*Pharmaceutical Chemistry Department, Faculty of Pharmacy, Heliopolis University for Sustainable Development, Cairo, Egypt. E-mail: eladlkhaled74@azhar.edu.eg; khaled.eladl@hu.edu.eg; eladlkhaled74@yahoo.com; nada.aziz@hu.edu.eg*

[b]*Pharmaceutical Chemistry Department, Faculty of Pharmacy, Cairo University, Cairo 11562, Egypt. E-mail: walaa.abozaid@pharma.cu.edu.eg*

[c]*Pharmaceutical Chemistry Department, Faculty of Pharmacy, Al-Azhar University, Cairo, Egypt*

† Electronic supplementary information (ESI) available. See https://doi.org/10.1039/d2ra01119k

is the VEGF passageway. VEGF signaling plays an important role in neoangiogenesis, and its blocking is a key curative strategy in cancer treatment.[5] During oncogenesis and acquired therapeutic resistance VEGF and EGF may function exclusively of one another where they share common downstream signaling pathways. It has been suggested that EGFR-mutant tumors are more VEGF-dependent than EGFR wild-type tumors.[9] Therefore, mutual VEGF and EGFR inhibition represent a rational combination strategy for EGFR-mutant NSCLC treatment.

VEGFR-2 is the fundamental regulator of VEGF-driven responses in endothelial cells and can control proliferation, differentiation, and microvascular permeability. Over and above, it has shown to be a prerequisite signal transducer in both physiologic and pathologic angiogenesis.[10] VEGFR-2 is overexpressed in several malignancies, including hepatocellular carcinoma, breast, colorectal, ovarian and thyroid cancer, melanoma and medulloblastoma.[11] Therefore, VEGFR-2 has been identified as an excellent therapeutic target for the production of novel anticancer agents.[12] Numerous TZD derivatives, were reported to be potent anticancer agents and inhibitors of angiogenesis targeting VEGFR-2 *via* decreasing the VEGF production in an *in vitro* model *e.g.* ciglitazone **I**[13] compound (**II**).[9] Due to the important role of VEGFR-2 in angiogenesis, this receptor is the most vital target in anti-angiogenic therapy against cancer. A number of effective VEGFR-2 inhibitors have been established and permitted as antiangiogenic drugs for treatment of numerous cancers, *e.g.* sunitinib (**III**)[14] and sorafenib (Nexavar)® (**IV**)[15] (Fig. 1).

Moreover, numerous TZD derivatives were reported to be potent EGFR inhibitors.[16] Overexpression of EGFR-tyrosine kinaseis common in many human solid tumors[17] as breast cancer[18] and hepatocellular carcinoma (HCC).[19] Therefore, EGFR-TK is considered as a rational target for the design of new anticancer agents.[20]

VEGFR-2 and EGFR are involved in the progression of different kinds of tumors and pathological disorders. They are closely related and sharing partial common downstream signaling pathways. The functional relationship between VEGFR-2 and EGFR has been well-recognized: antitumor effect of EGFR inhibitors was increased by VEGFR-2 signaling pathway inhibition, while activation of VEGFR-2 independent of EGFR signaling may give rise to the resistance of EGFR inhibitors.[21] Thus, the simultaneous blockade of both EGFR and VEGFR signaling pathways appears to be an attractive methodology to cancer therapy.[22]

VEGFR-2 inhibitors can be categorized into three types. Type I inhibitors that occupy the ATP binding region forming a hydrogen bond with the hinge region amino acid Cys919. Type II inhibitors are occupying the ATP binding site and extend over the gate area into the adjacent allosteric hydrophobic back pocket. Type III inhibitors that block the receptor through hydrophobic interactions and they accommodate the allosteric hydrophobic back pocket of VEGFR-2. The affinity and selectivity of the type II inhibitors are preferred over type I inhibitors. Moreover, type II inhibitors increase their drug-target residence time so prolong TK suppression.[23] Therefore, diverse strategies have been employed to develop novel type II VEGFR-2 inhibitors (Fig. 2A).

Moreover, the ATP binding pocket of EGFR-TK consists of five main regions; (a) adenine binding pocket contains key amino acids which can form hydrogen bonds with the adenine ring, (b) sugar region (hydrophilic ribose pocket), (c) hydrophobic region I, plays an important role in inhibitor selectivity, (d) hydrophobic region II, may be exploited for inhibitor specificity, (e) phosphate binding region that can be used for improving inhibitor pharmacokinetics (Fig. 2B).[24]

In continuation of our preceding efforts toplot and synthesis new anticancer agents[25–32] we designed and synthesized novel thiazolidine-2,4-diones bearing heterocyclic rings as dual VEGFR-2/EGFR-mutant tyrosine kinase inhibitors for treatment of NSCLC lung (A549), hepatocellular carcinoma (HCC) type (HepG2), breast cancer (michigan cancer foundation-7 (MCF-7)) and human colorectal carcinoma-116 (HCT-116).

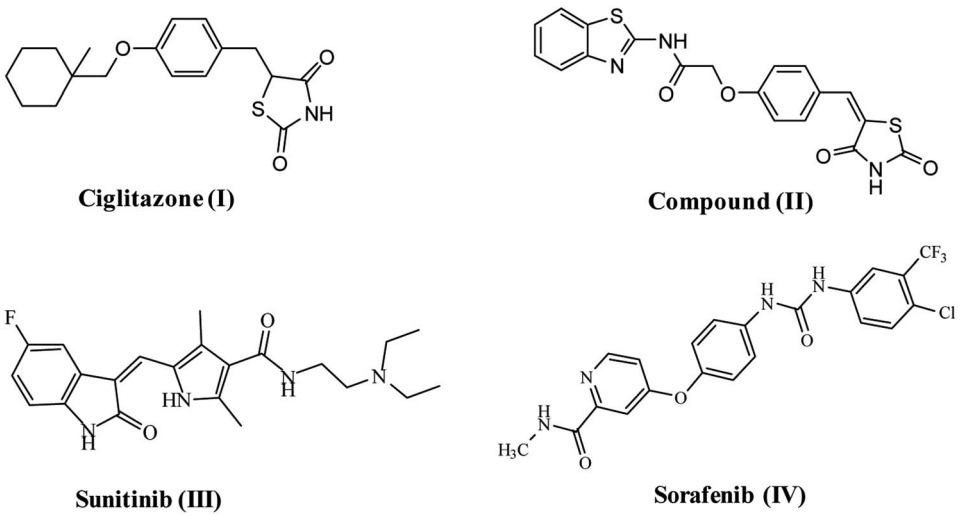

Fig. 1 Reported VEGFR-2 inhibitors.

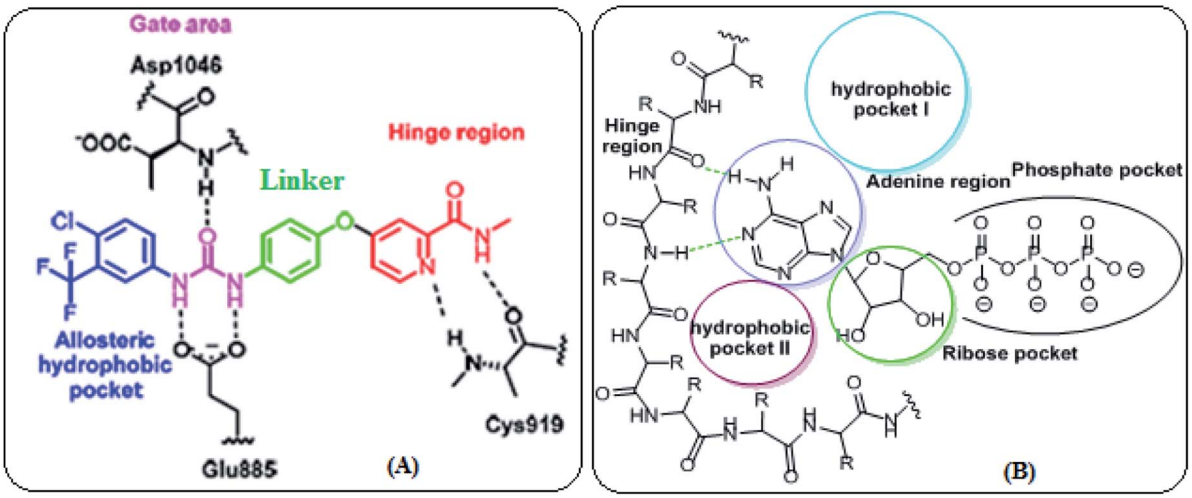

Fig. 2 (A) VEGFR-2 active site (B) EGFR-TK active site.

1.1. Rationale and structure-based design

Our idea in the rational of our derivatives comes from that our derivatives showed the required pharmacophoric features of both EGFR and VEGFR-2 inhibitors (Fig. 3). Sorafenib and multiple VEGFR-2 inhibitors had four main features:[33,34] (i) a flat hetero aromatic ring which occupied the adenosine triphosphate (ATP)-binding domain.[34] (ii) A central hydrophobic spacer.[35] (iii) A linker containing a functional group (*e.g.* amino or urea) that possesses both H-bond acceptor (HBA) and donor (HBD) in order to bind along with two crucial residues (Glu885 and Asp1046). The NH motifs of the urea or amide moiety commonly make one hydrogen bond with Glu885, whereas the C═O motif forms a further hydrogen bond with Asp1046.[36] (iv) The terminal hydrophobic moiety that occupies the allosteric hydrophobic pocket[37] (Fig. 3A).

The main core of our molecular design rationale was carried out by bioisosteric modification strategies of VEGFR-2 inhibitors (sorafenib & sunitinib) at four different positions (Fig. 3A).

In addition, the common pharmacophoric features of EGFR-TKIs are: (i) terminal hydrophobic head to be inserted in the hydrophobic region I. (ii) A flat hetero aromatic system, occupying the adenine binding pocket. This hetero aromatic system can participate in hydrogen bonding interactions with Met793, Thr854,and Thr790 residues[38] (iii) NH spacer which can form important hydrogen bond interaction to amino acid residues in the linker region. (iv) Hydrophobic tail which occupies the hydrophobic region II.[39]

In this work, a series of thiazolidine-2,4-diones derivations having the fundamental pharmacophoric characters of EGFR-TKIs have been framed and synthesized. Such compounds comprised structural modification of elotinib at four different positions (Fig. 3B).

As VEGFR-2 inhibitors the first bioisosteric modification was adopted in the target furan and/or thiophene rings to replace the pyridine and 5-fluoro-2-oxoindolin-3-ylidene moieties of the reference ligands sorafenib and sunitinib, respectively. The second strategy is to use thiazolidine-2,4-dione to replace the central aryl and the five membered pyrrole rings of the reference ligands sorafenib and sunitinib, respectively aiming to increase VEGFR-2 binding affinity. The third strategy is using acetamide linkers containing HBA-HBD functional groups that possess H-bond acceptors and/or donors. In addition, the forth strategy where the hydrophobic diethylamino and 4-chloro-3-(trifluoromethyl)phenyl tail of sorafenib and sunitinib correspondingly, was replaced by phenyl one 4-substituted with different electronic and lipophilic environments (Fig. 4A).

As EGFR inhibitors the first position was the quinazoline moiety (hetero aromatic system), which was replaced by thiazolidine-2,4-dione ring as a biological isostere to occupy the adenine binding region. The second position was the terminal phenyl ring (hydrophobic head), where phenyl group with various substituents was used. The third position was the NH linker, where acetamide linker was utilized. The fourth position was the two 2-methoxyethoxy groups (hydrophobic tail), where thiophen-2-yl/furan-2-ylmethylene were incorporated at position-5 of thiazolidin-2,4-dione nucleus to be fitted in the hydrophobic region II of ATP binding site (Fig. 4B).

All modifications encouraged us to study the structure–activity relationship of the hypothesized compounds as anticancer agents. The most active structures were examined for their anti-proliferative activities against a number of human cancer cell lines. Promising compounds were examined for their activities against VEGFR-2 and EGFR^{T790M}. Furthermore, a molecular docking was performed to rationalize and emphasize the mechanism of action of the produced compounds as VEGFR-2 and EGFR-TKIs.

2. Results and discussion

2.1. Chemistry

The synthetic strategy for preparation of the target compounds **4a–g** and **5a–g** is depicted in Scheme 1. Synthesis was initiated by cyclocondensation of thiourea with chloroacetic acid to afford thiazolidine-2,4-dione (**1**)[27] which underwent further

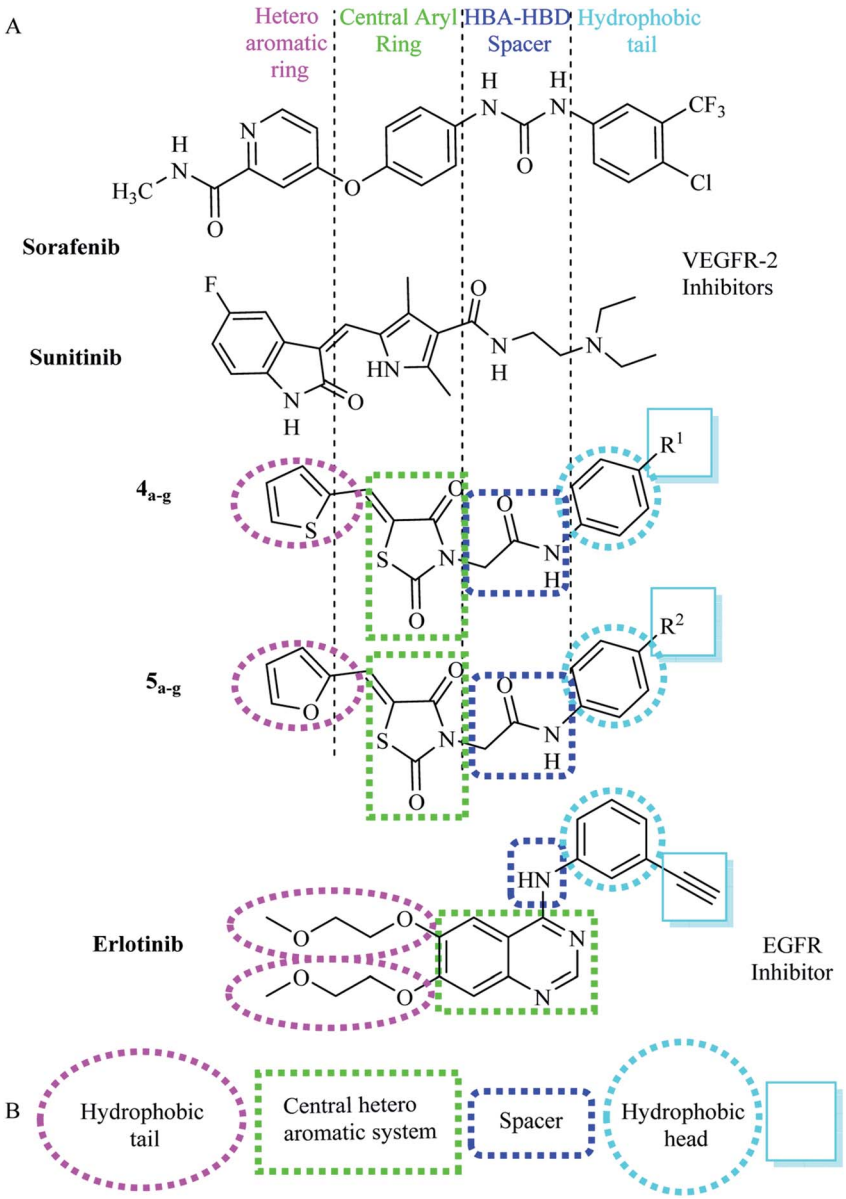

Fig. 3 (A) Basic structural features of EGFR inhibitors. (B) Basic structural features of VEGFR-2 inhibitors.

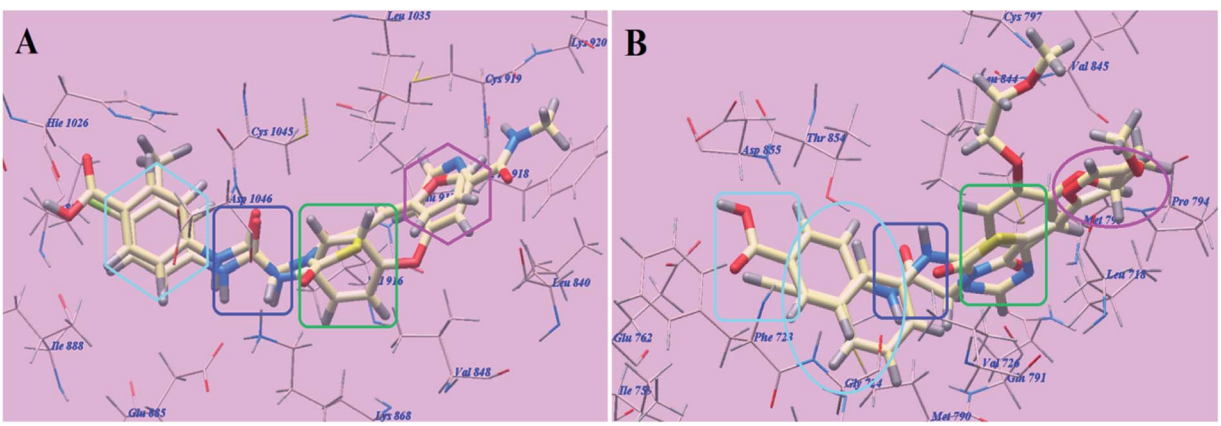

Fig. 4 (A) Superimposition of **5g** and sorafenib. (B) Superimposition of **5g** and elotinib.

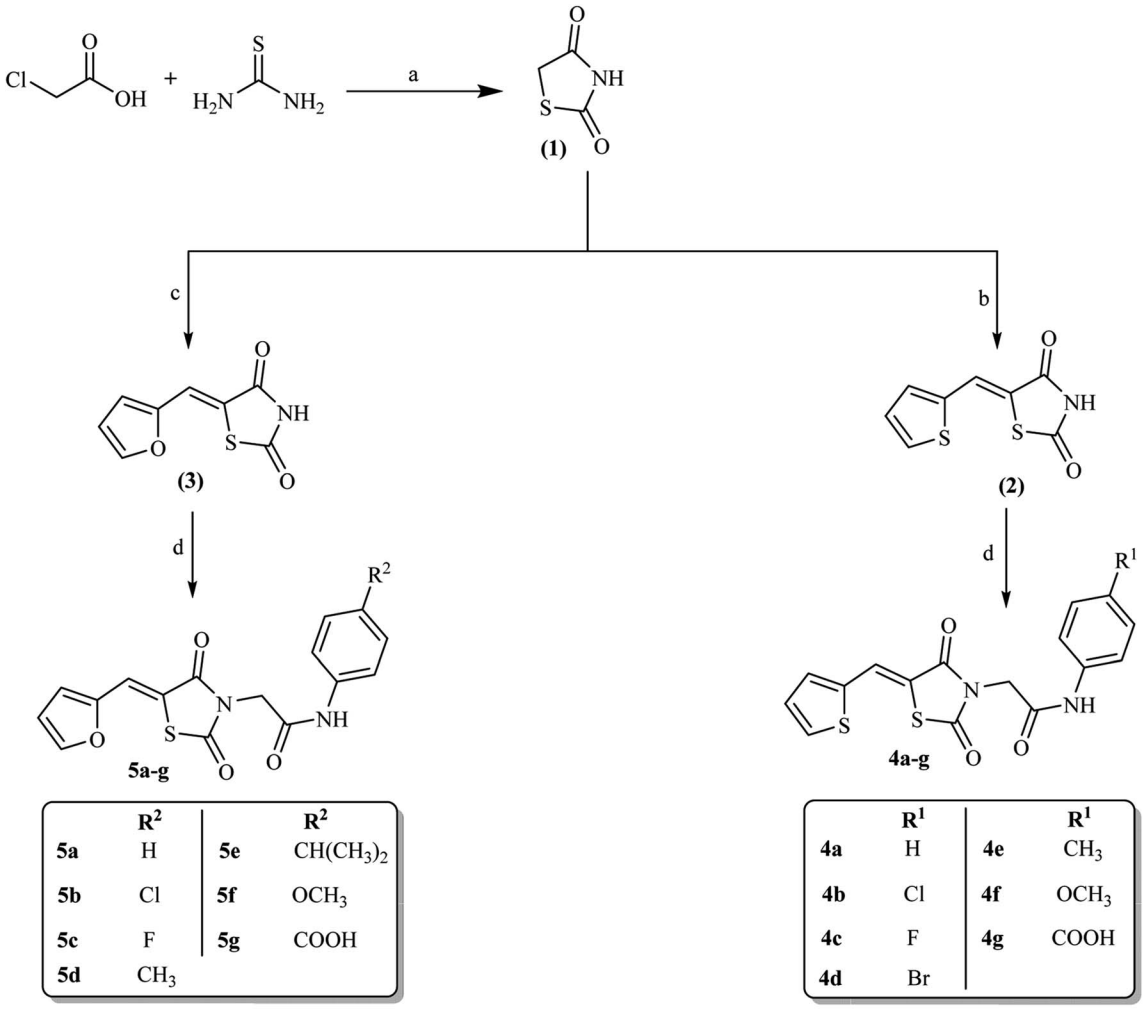

	R^2		R^2
5a	H	**5e**	$CH(CH_3)_2$
5b	Cl	**5f**	OCH_3
5c	F	**5g**	COOH
5d	CH_3		

	R^1		R^1
4a	H	**4e**	CH_3
4b	Cl	**4f**	OCH_3
4c	F	**4g**	COOH
4d	Br		

Scheme 1 Synthetic route for preparation of the target compounds **4a–g** and **5a–g**.

condensation reaction with thiophene-2-carbaldehyde and/or furan-2-carbaldehyde *via* Knoevenagel condensation[27] to afford 5-(thiophen-2-ylmethylene)thiazolidine-2,4-dione **2** and 5-(furan-2-ylmethylene)thiazolidine-2,4-dione **3** respectively. Subsequent heating of **2** and **3** under reflux with the appropriate chloroacetamide derivative in acetone in the presence of potassium carbonate afforded the corresponding amide derivatives **4a–g** and **5a–g** correspondingly.

It is advantageous to state that there is no risk for a nitrosamine formation in our derivatives. The nitrosamine formation on the amino NH group depends on the presence of nitrosating agent, basicity of NH group and the steric accessibility to the nitrogen atom.[40] As our derivatives containing electron withdrawing group attached to NH group (forming amide linkers) and also NH attached to electron with drawing benzene ring directly so the electrons on the NH groups is not available to be donated to attack or form nitrosamine. Moreover, there is highly steric hindrance to reach to the NH atom as it lies between two bulky thiazolidine-2,4-dione and phenyl groups.

2.2. Docking studies

Molsoft software was applied for molecular docking studies. All experiments utilized VEGFR-2 and $EGFR^{T790M}$ (PDB ID 4ASD)[40] and (PDB ID 3W2O)[39] respectively.

2.2.1. Docking studies as VEGFR-2 inhibitors. The achieved outcomes showed that all the studied congeners have identical position and orientation inside the recognized binding site of VEGFR-2 that reveals a large space bounded by a membrane-binding domain, which serves as entry channel for substrate to the active site (Fig. 5). The binding free energy (ΔG) explained that most of these compounds had good receptor binding affinity (Table 1).

Sorafenib suggested binding mode showed affinity value -99.50 kcal mol^{-1} and formed 5 H-bonds. It formed 2 H-

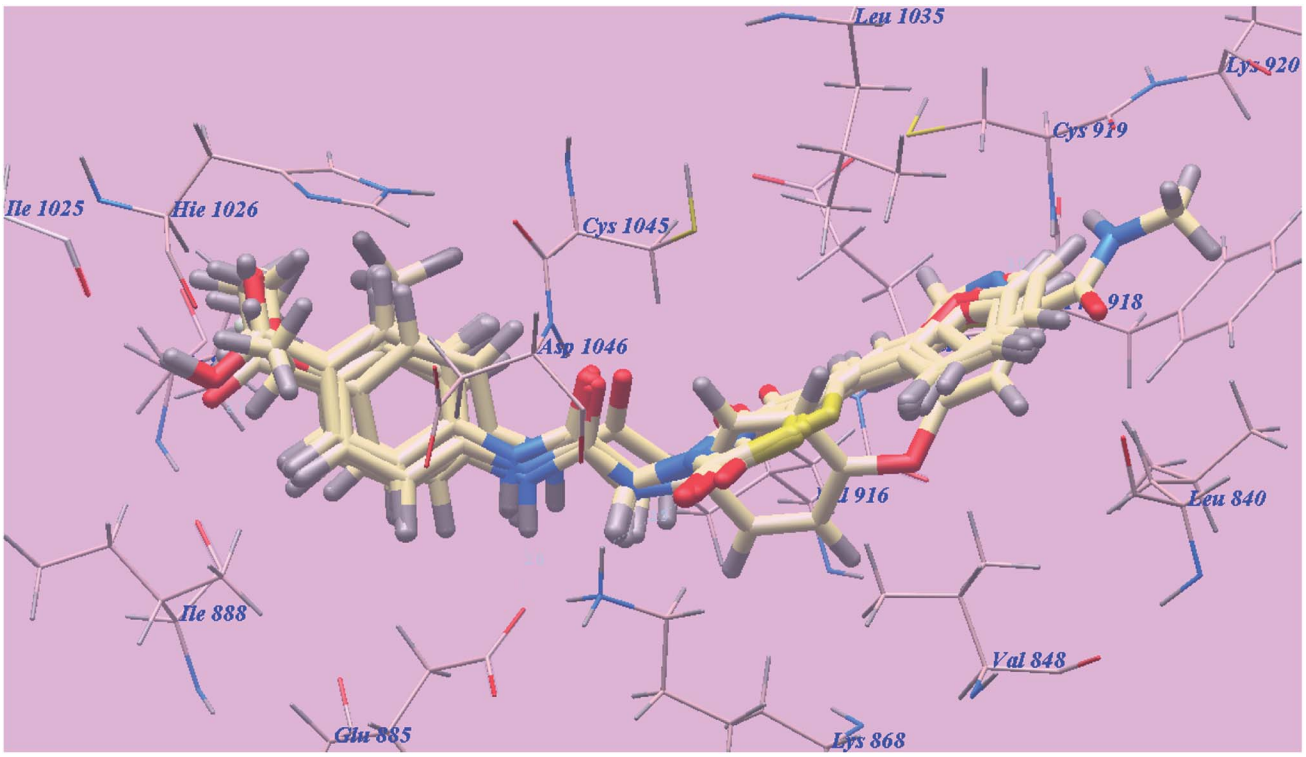

Fig. 5 Superimposition of some docked compounds inside the binding pocket of 4ASD.

Table 1 The calculated free energy (ΔG in kcal mol^{-1}) of ligands binding with VEGFR-2

Compound	ΔG [kcal mol^{-1}]	Compound	ΔG [kcal mol^{-1}]
4a	−84.77	**5b**	−88.80
4b	−87.36	**5c**	−89.65
4c	−88.18	**5d**	−91.06
4d	−91.36	**5e**	−90.52
4e	−89.77	**5f**	−99.85
4f	−91.24	**5g**	−102.80
4g	−100.12	Sorafenib	−99.50
5a	−85.04		

bonding interactions with *Cysteine919* (2.51 Å and 2.10 Å), 2 H-bonds with *Glutamate885* (1.77 Å and 2.75 Å) and one H-bonding interaction with *Aspartate1046* (1.50 Å). The *N*-methylpicolinamide group occupied the pocket made *via* *Leucine1035*, *Lysine920*, *Cysteine919*, *Phenylalanine918*, *Glutamate917*, *Valine848* and *Leucine840*. Furthermore, the central phenyl linker occupied the hydrophobic groove made by *Cysteine1045*, *Leucine1035*, *Threonine916*, *Lysine868* and *Valine848*. Additionally, the terminal 3-trifluromethyl-4-chlorophenyl group occupied the hydrophobic channel formed by *Aspartate1046*, *Cysteine1045*, *Histidine1026*, *Isoleucine892*, *Isoleucine888* and *Glutamate885* (Fig. 6). The urea linker had a significant function in the binding with VEGFR-2 enzyme; however, the linker had important role responsible for high binding affinity of sorafenib. These conclusions promote us to use acetamide linker wishing to get effective VEGFR-2 inhibitors.

The proposed binding mode of compound **5g** is virtually the same as that of sorafenib which revealed affinity value of −102.80 kcal mol^{-1} and 5 H-bonds. The furan ring formed one H-bond with *Cysteine919* (2.98 Å). The carbonyl group of the acetamide linker formed one H-bond with *Aspartate1046* (1.41 Å) while its NH group formed another H bond with *Glutamate885* (2.22 Å). The carbonyl group at position-2 of thiazolidine-2,4-dione formed one H-bond with *Lysine868* (2.13 Å). Furthermore, the OH group of the distal carboxylic acid moiety formed one H-bond with *Arginine1025* (2.23 Å). The heterocyclic furan ring occupied the pocket made by *Leucine1035*, *Cysteine919*, *Phenylalanine918*, *Glutamate917*, *Valine848* and *Leucine840*. Furthermore, the thiazolidine-2,4-dione linker occupied the hydrophobic groove made by *Cysteine1045*, *Leucine1035*, *Threonine916*, *Lysine868* and *Valine848*. Additionally, the terminal phenyl tall occupied the hydrophobic channel formed by means of*Aspartate1046*, *Cysteine1045*, *Histidine1026*, *Isoleucine892*, *Isoleucine888* and *Glutamate885* (Fig. 7). These interactions of compound **5g** may explain the highest anticancer activity.

The proposed binding mode of compound **4g** is virtually the same as that of sorafenib and **5g** which revealed affinity value of −100.12 kcal mol^{-1} and 4 H-bonds. The carbonyl group of the acetamide linker formed 1 H-bond with *Aspartate1046* (1.37 Å) while its NH group formed another H bond with *Glutamate885* (2.27 Å). The carbonyl group at position-2 of thiazolidine-2,4-dione formed one H-bond with *Lysine868* (2.11 Å).

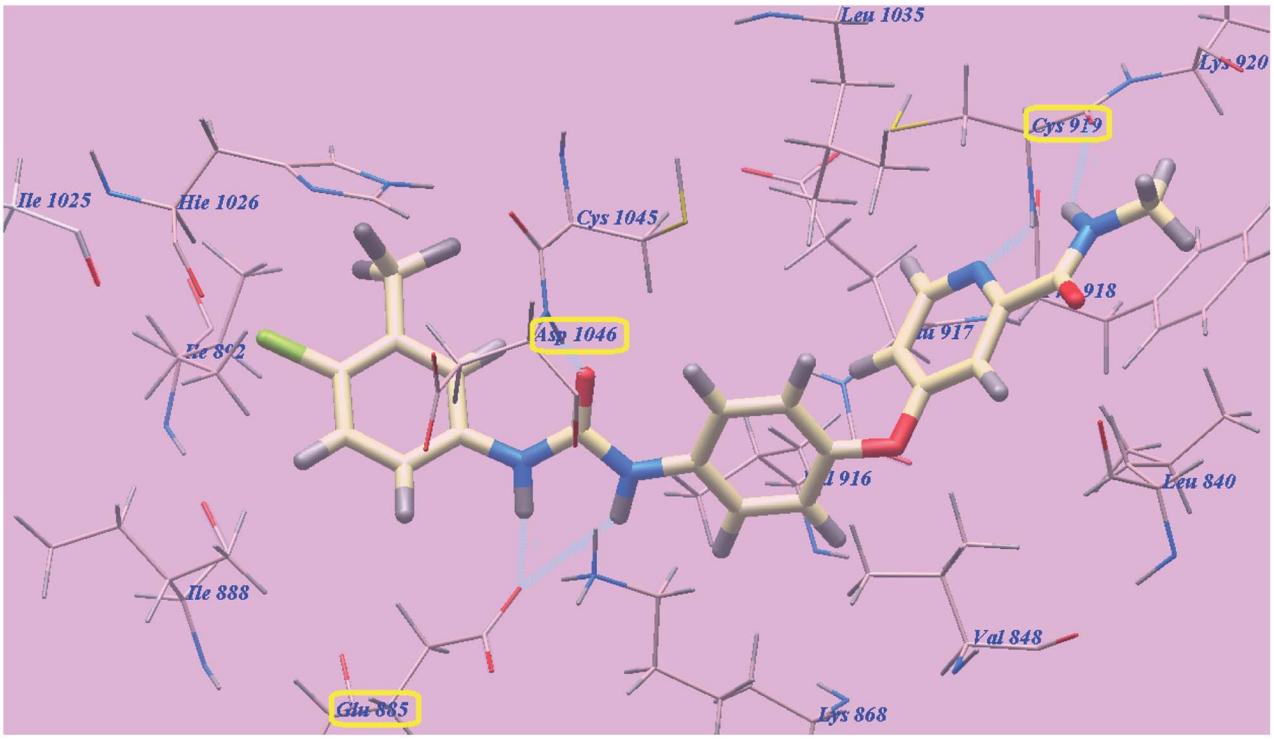

Fig. 6 Predicted binding mode for sorafenib with 4ASD. H-bonded atoms are indicated by dotted lines.

Furthermore, the OH group of the distal carboxylic acid moiety formed 1 H-bond with *Arginine1025* (2.63 Å). The heterocyclic thiophene ring occupied the pocket made by *Leucine1035*, *Cysteine919*, *Phenylalanine918*, *Glutamate917*, *Valine848* and *Leucine840*. Furthermore, the thiazolidine-2,4-dione linker occupied the hydrophobic groove made by *Cysteine1045*,

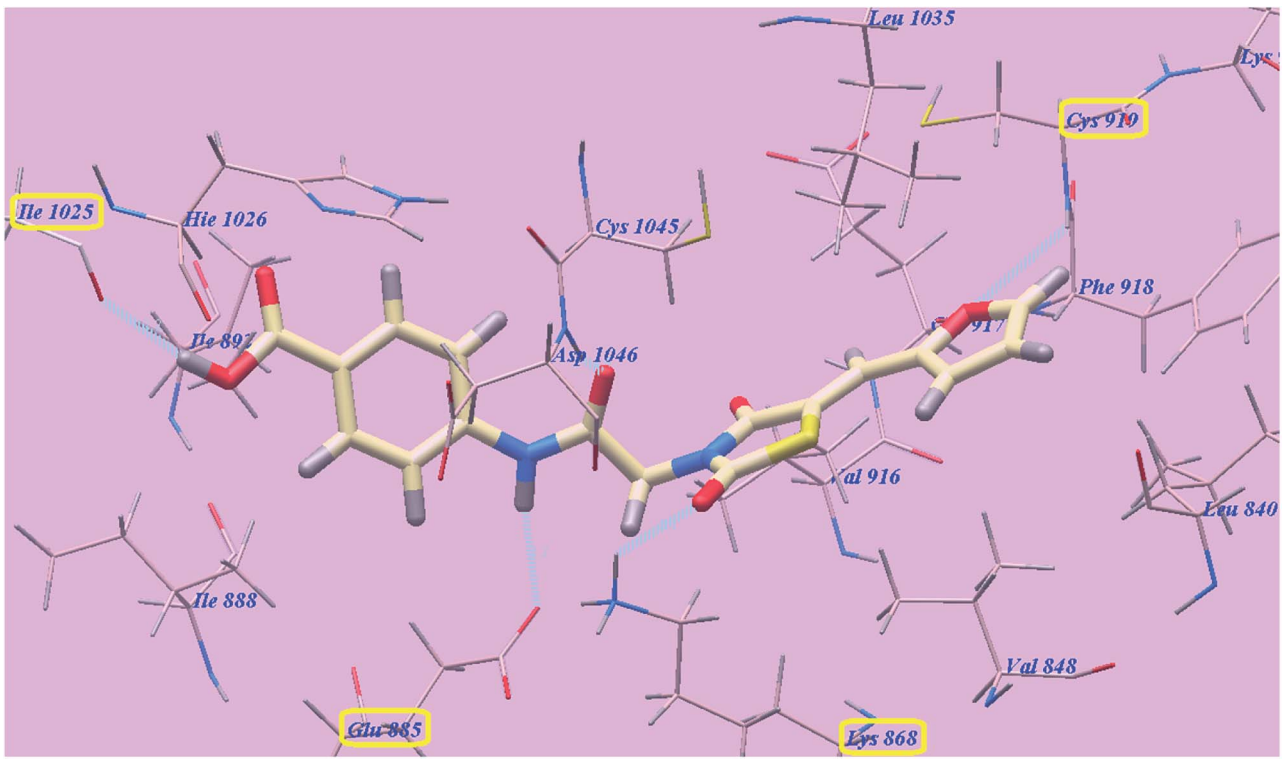

Fig. 7 Predicted binding mode for **5g** with 4ASD.

Leucine1035, *Threonine916*, *Lysine868* and *Valine848*. Additionally, the terminal phenyl tall occupied the hydrophobic channel formed by *Aspartate1046*, *Cysteine1045*, *Histidine1026*, *Isoleucine892*, *Isoleucine888* and *Glutamate885* (Fig. 8). These interactions of compound **4g** may explain its high anticancer activity.

The proposed binding mode of compound **5f** is virtually the same as that of **5g** with affinity value of −99.85 kcal mol^{-1} and 4 H-bonds (Fig. 9).

From the accomplished docking results (Table 1), we concluded that, the acetamide linker occupied the same groove occupied by urea linker of sorafenib and played the same role which is essential for higher affinity towards VEGFR-2 enzyme. The heterocyclic furan ring increased affinities towards VEGFR-2 enzyme than the heterocyclic thiophene one. This may due to formation of H-bond with the oxygen of the furan ring with *Cysteine919*. The carbonyl group at position-2 of thiazolidine-2,4-dione derivatives form new H-bond with the amino acid *Lysine866*.

2.2.2. Docking studies as EGFR^{T790M} inhibitors. The achieved results showed that all studied congeners have similar position and orientation inside the recognized binding site of EGFR that reveals a large space bounded by a membrane-binding domain, which serves as entry channel for substrate to the active site (Fig. 10). The picked up results of the free energy of binding (ΔG) explained that most of these compounds had good binding affinity toward the receptor and the computed values reflected the overall trend (Table 2).

The proposed binding mode of elotinib unveiled affinity value of −82.77 kcal mol^{-1} and 4 H-bonds. One of the two 2-methoxyethoxy groups formed one H-bond with the inhabitant amino acid *Cysteine797* (2.05 Å). The quinazoline moiety was stabilized by formation of two H bonds with *Methionine793* (1.82 Å) and *Valine726* (2.97 Å). The NH spacer formed one H-bond with the essential amino acid *Threonine854* (2.99 Å). The 3-ethynylphenyl head occupied the hydrophobic region I formed by *Aspartate855*, *Threonine854*, *Glutamine791*, *Methionine790*, *Leucine777*, *Glutamate762*, *Isoleucine759*, *Valine726*, *Glycine724* and *Phenylalanine723*. Moreover, the 2-methoxyethoxy tail occupied the hydrophobic region II formed through *Valine845*, *Leucine844*, *Proline794*, *Methionine793* and *Leucine718* (Fig. 11).

The proposed binding mode of compound **5g** is virtually the same as that of elotinib that showed affinity value of −81.06 kcal mol^{-1} and 4 H-bonds. The carbonyl group of the acetamide linker formed 1 H-bond with the chief amino acid *Threonine854* (2.78 Å). The carbonyl group at position-4 of thiazolidine-2,4-dione formed 1 H-bond with *Methionine793* (2.02 Å). Moreover, the carboxylate group at position-4 of the phenyl tail was stabilized by formation of two H-bonds with *Aspartate855* (2.61 Å) and *Glutamate762* (2.61 Å). The terminal phenyl group occupied the hydrophobic region I formed by *Aspartate855*, *Threonine854*, *Glutamine791*, *Methionine790*, *Leucine777*, *Glutamate762*, *Isoleucine759*, *Valine726*, *Glycine724* and *Phenylalanine723*. Moreover, the heterocyclic furan ring occupied the hydrophobic region II formed by *Valine845*, *Leucine844*, *Proline794*, *Methionine793* and *Leucine718* (Fig. 12). These interactions of compound **5g** may explain the highest anticancer activity.

The proposed binding mode of compound **4g** is virtually the same as that of elotinib and **5g** revealed affinity value of −77.08 kcal mol^{-1} and 4 H-bonds. The carbonyl group of the acetamide linker formed one H-bond with the key amino acid

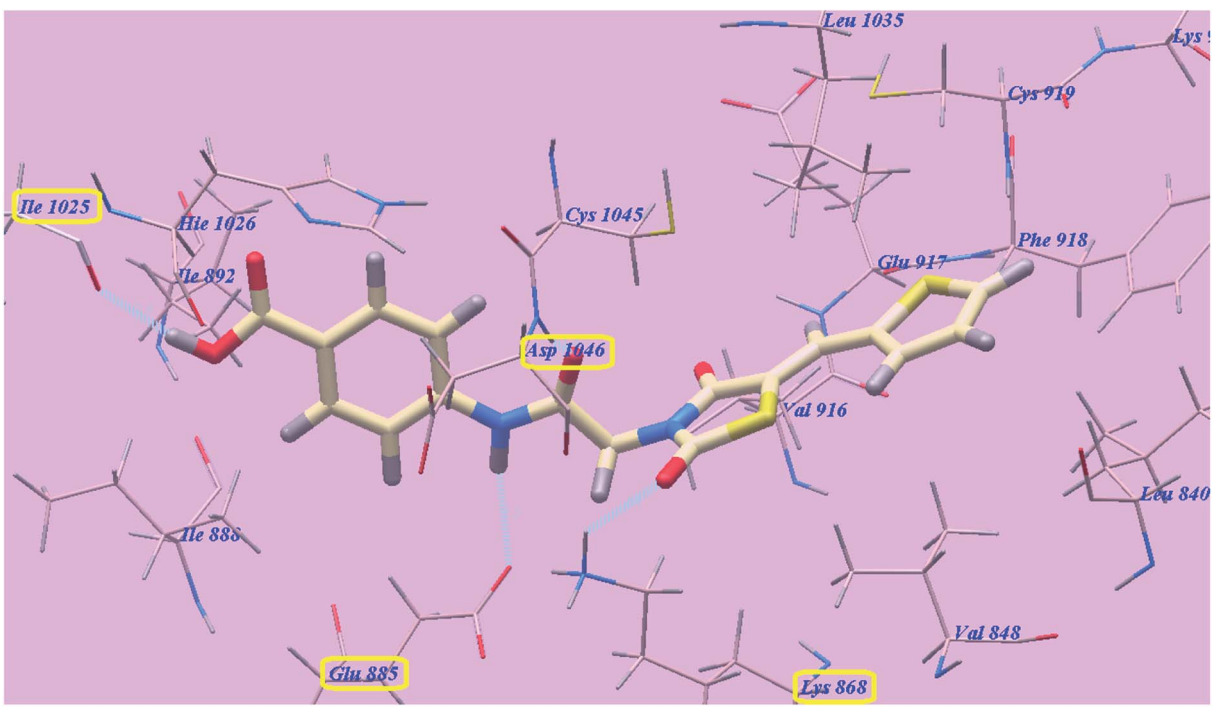

Fig. 8 Predicted binding mode for **4g** with 4ASD.

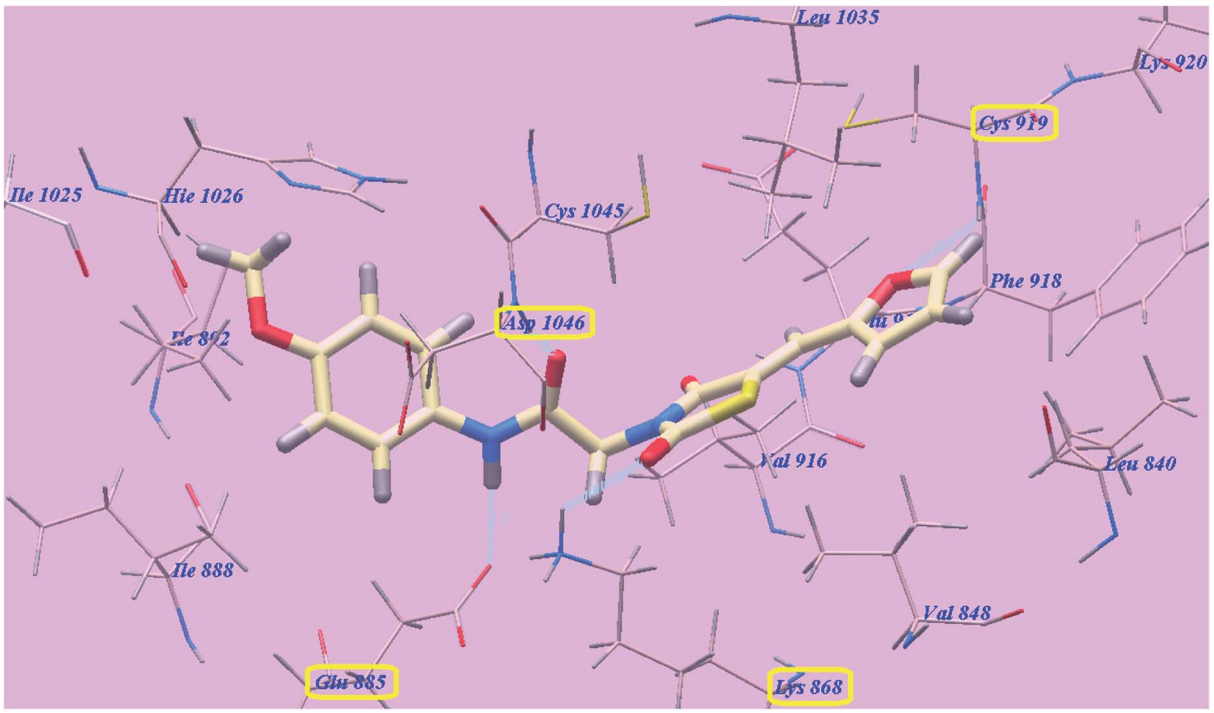

Fig. 9 Predicted binding mode for **5f** with 4ASD.

Threonine854 (2.77 Å). The carbonyl group at position-4 of thiazolidine-2,4-dione formed one H-bond with *Methionine793* (2.04 Å). Moreover, the carboxylate group at position-4 of the phenyl tail was stabilized by formation of two H-bonds with *Aspartate855* (2.60 Å) and *Glutamate762* (2.62 Å). The terminal phenyl group occupied the hydrophobic region I formed by *Aspartate855*, *Threonine854*, *Glutamine791*, *Methionine790*, *Leucine777*, *Glutamate762*, *Isoleucine759*, *Valine726*,

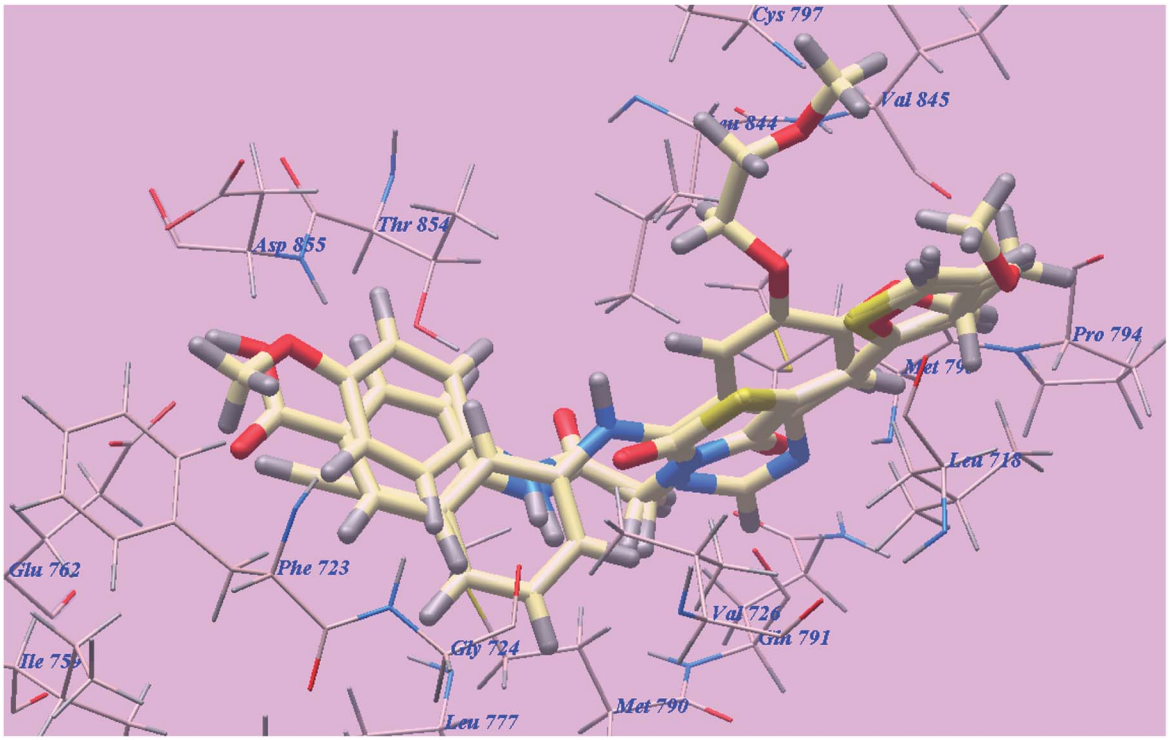

Fig. 10 Superimposition of some docked compounds inside the binding pocket of 3W2O.

Table 2 The calculated free energy (ΔG in kcal mol^{-1}) of ligands binding with EGFR^{T790M}

Compound	ΔG [kcal mol^{-1}]	Compound	ΔG [kcal mol^{-1}]
4a	−65.49	**5b**	−74.50
4b	−73.10	**5c**	−74.49
4c	−68.41	**5d**	−72.15
4d	−74.45	**5e**	−77.02
4e	−68.13	**5f**	−73.60
4f	−71.89	**5g**	−81.06
4g	−77.08	Erlotinib	−82.77
5a	−66.09		

Glycine724 and *Phenylalanine723*. Moreover, the heterocyclic thiophene ring occupied the hydrophobic region II formed by *Valine845*, *Leucine844*, *Proline794*, *Methionine793* and *Leucine718* (Fig. 13).

The proposed binding mode of compound **4f** is virtually the same as that of **4g** and revealed affinity value of −71.89 kcal mol^{-1} and 3 H-bonds with *Threonine854* (2.71 Å), *Methionine793* (2.20 Å) and *Aspartate855* (2.96 Å). The terminal 4-methoxyphenyl group occupied the hydrophobic region I formed by *Aspartate855*, *Threonine854*, *Glutamine791*, *Methionine790*, *Leucine777*, *Glutamate762*, *Isoleucine759*, *Valine726*, *Glycine724* and *Phenylalanine723*. Moreover, the heterocyclic thiophene ring occupied the hydrophobic region II formed by *Valine845*, *Leucine844*, *Proline794*, *Methionine793* and *Leucine718* (Fig. 14).

2.3. *In vitro* cytotoxic activity

Anti-proliferative action of the newly prepared 5-benzylidenethiazolidine-2,4-dione derivatives $\mathbf{4_{a–g}}$–$\mathbf{5_{a–g}}$ was examined *versus* four human tumor cell lines namely, hepatocellular carcinoma (HepG2), lung cancer (A549), breast cancer (MCF-7) and colorectal carcinoma (HCT-116) using 3-[4,5-dimethylthiazol-2-yl]-2,5-diphenyltetrazolium bromide (MTT) colorimetric assay as described by Mosmann.[41,42] Sorafenib and elotinib were included in the experiments as reference cytotoxic drugs. The results were expressed as growth inhibitory concentration (IC_{50}) values and summarized in Table 3. From the obtained results, it was explicated that most of the prepared compounds showed excellent to modest growth inhibitory activity toward the tested cancer cell lines. In general, investigations of the cytotoxic activity indicated that HepG2 was the most liable cell line to the effect of the new derivatives. Especially, compounds **5g** and **4g** were observed to be the best effective compounds against HepG2 (IC_{50} = 3.86 and 6.22 μM), A549 (IC_{50} = 7.55 and 12.92 μM), MCF-7 (IC_{50} = 10.65 and 10.66 μM) and HCT116 (IC_{50} = 9.04 and 11.17 μM) tumor cell lines. Compound **5g** showed higher activities than sorafenib (IC_{50} = 4.00, 4.04, 5.58 and 5.05 μM) against HepG2 but lower activities *versus* A549, MCF-7 and HCT116 correspondingly. However, this structure demonstrated higher actions than elotinib (IC_{50} = 7.73, 5.49, 8.20 and 13.91 μM), toward HepG2 and HCT116 but lower activities *versus* both A549 and MCF-7 correspondingly. However compound **4g** presented lower activities than sorafenib against the four cell lines, it also demonstrated higher actions than elotinib against HepG2 and HCT116 but lower activities *versus* both A549 and MCF-7 correspondingly.

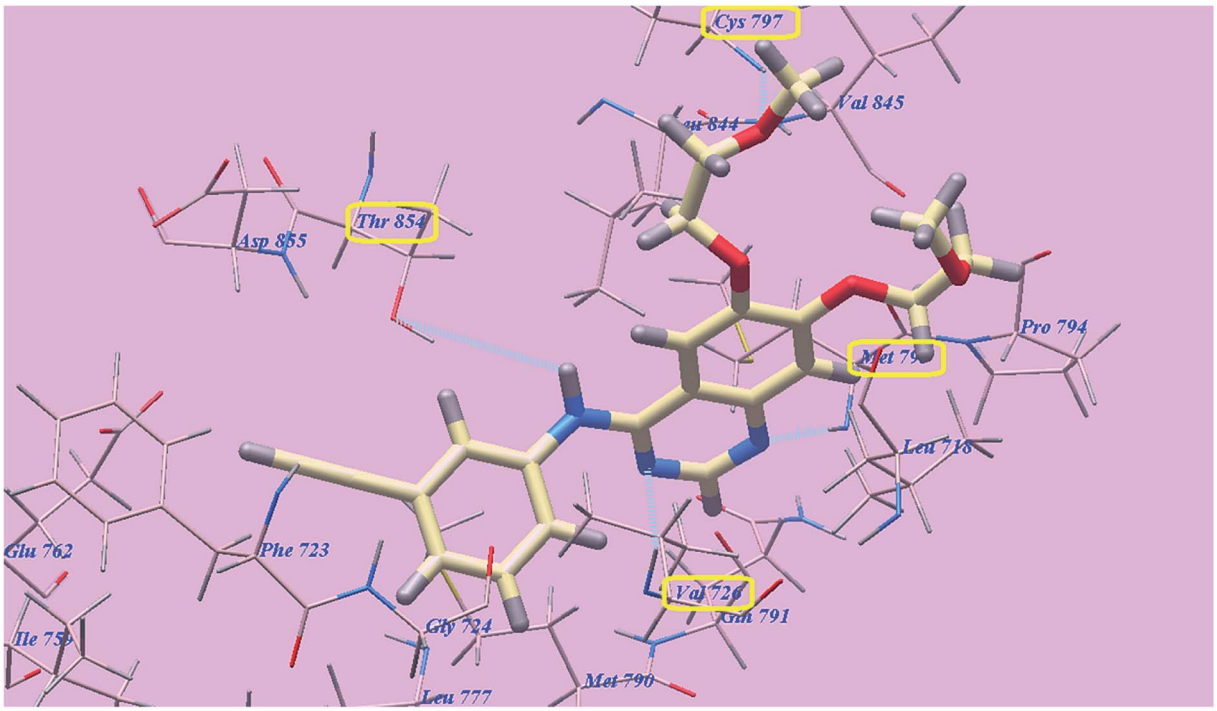

Fig. 11 Predicted binding mode for elotinib with 3W2O. H-bonded atoms are indicated by dotted lines.

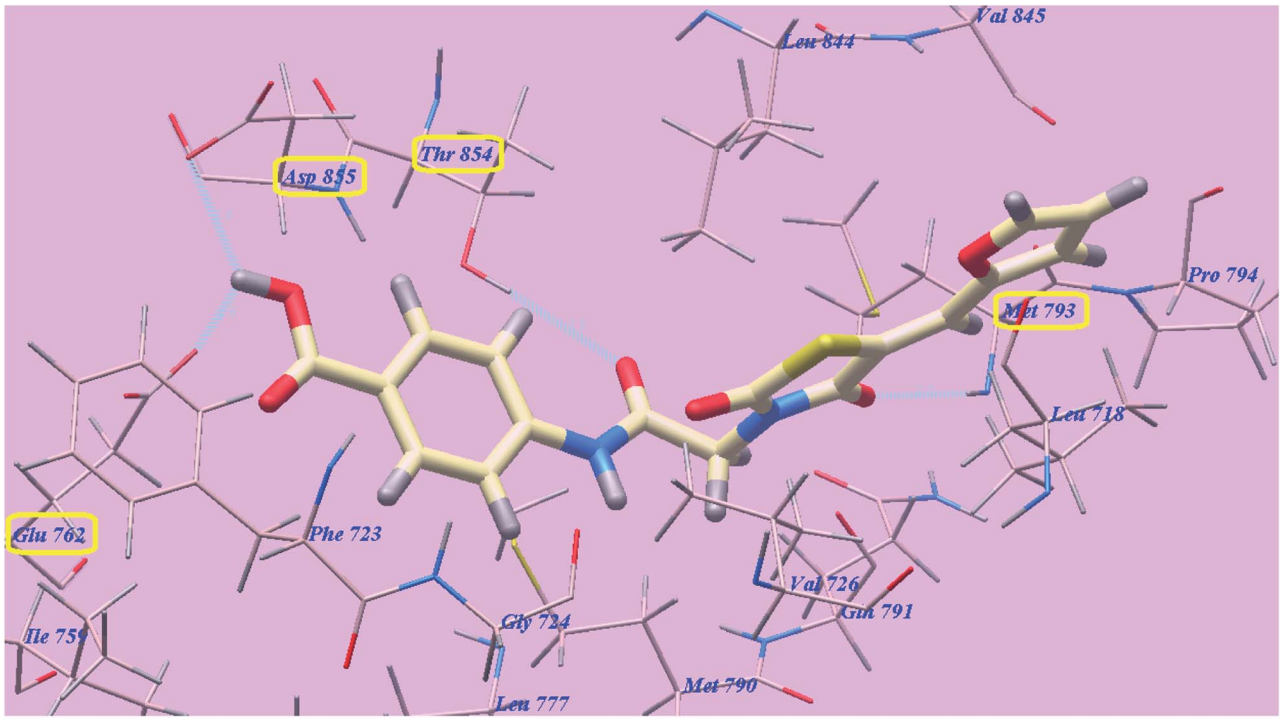

Fig. 12 Predicted binding mode for **5g** with 3W2O.

Regarding HepG2, compounds **4d**, **4e**, **4f**, **5b**, **5c**, **5d**, **5e** and **5f** exhibited the greatest anticancer effects with IC_{50} ranging from 10.24 to 24.54 μM. Derivatives **4b** and **4c** with $IC_{50} = 35.40$ and 34.23 μM consequently, showed good cytotoxicity. Derivatives **4a** and **5a** with the same $IC_{50} = 52.11$ μM exhibited moderate cytotoxicity.

Concerning A549, compounds **4d**, **4f** and **5f** exhibited the greatest anticancer effects with $IC_{50} = 18.97$, 22.73 and 13.02

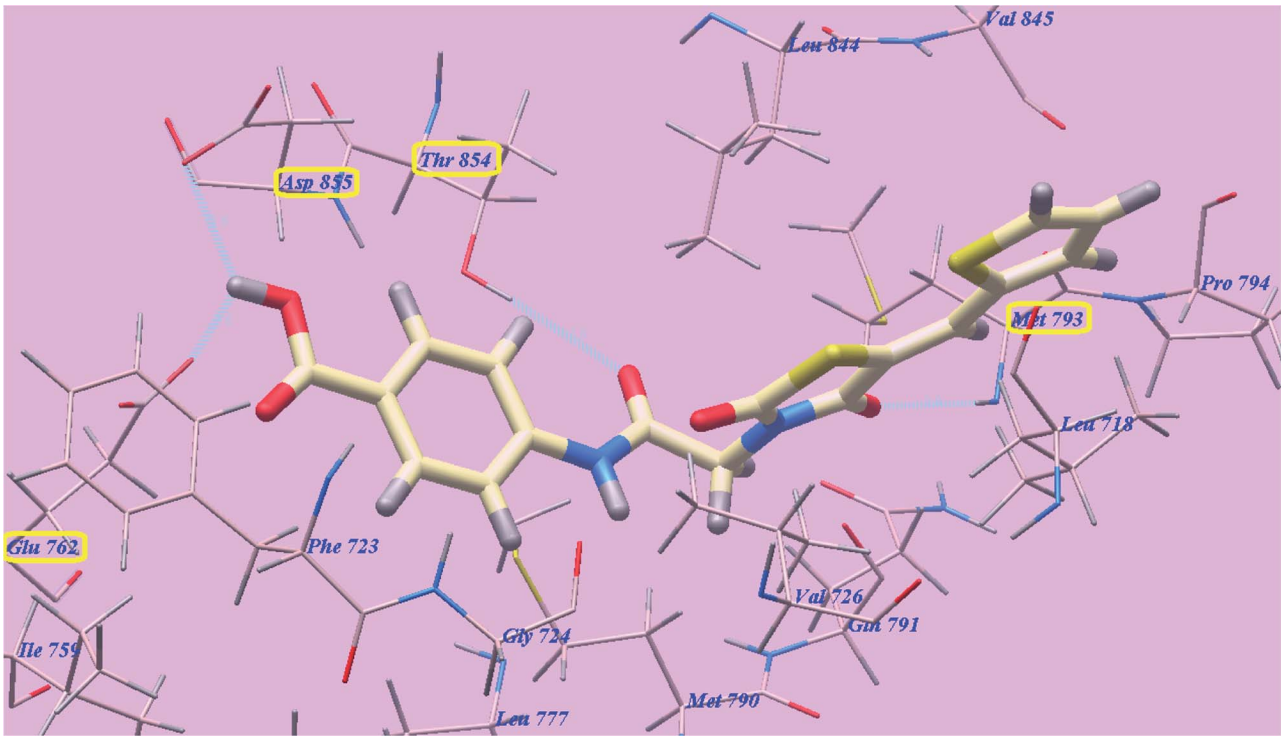

Fig. 13 Predicted binding mode for **4g** with 3W2O.

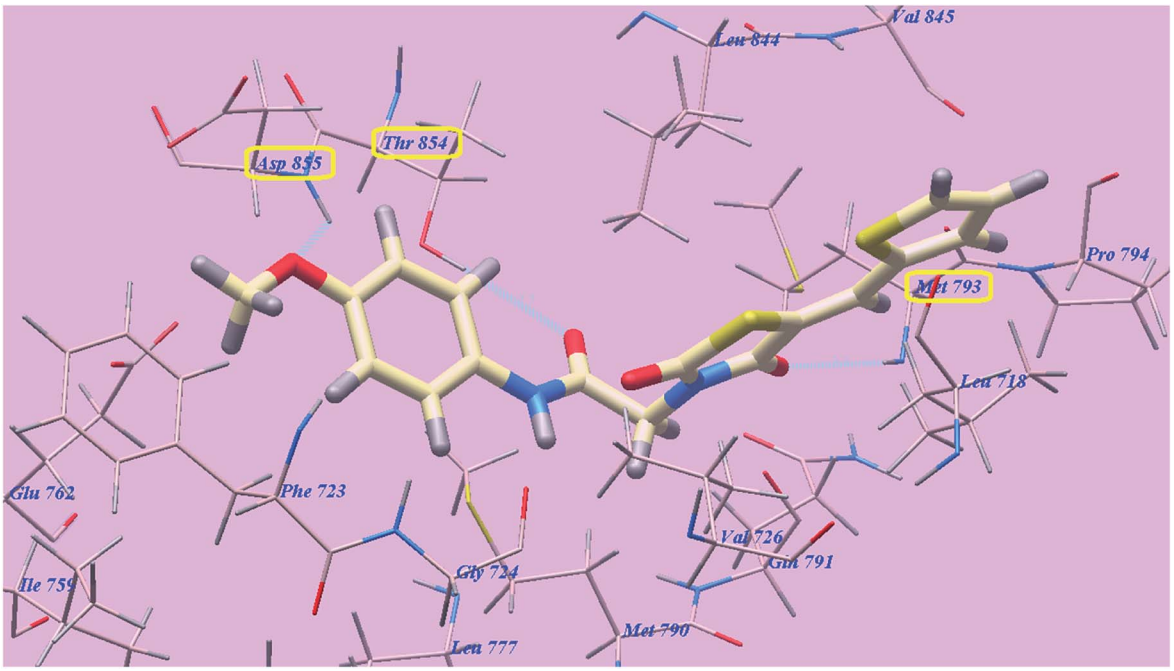

Fig. 14 Predicted binding mode for **4f** with 3W2O.

μM consequently. Derivatives **4b**, **4c**, **4e**, **5b**, **5c**, **5d** and **5e** with IC_{50} ranging from 29.66 to 38.32 μM, showed good cytotoxicity. Derivatives **4a**, and **5a** with IC_{50} = 51.00 and 53.22 μM exhibited moderate cytotoxicity.

Derivatives **4d**, **4f**, **5e** and **5f** exhibited the ultimate anticancer effect with IC_{50} = 22.73, 22.29, 14.54 and 18.53 μM correspondingly upon assessment against MCF-7. Derivatives **4b**, **4c**, **4e**, **5b**, **5c** and **5d** with IC_{50} ranging from 25.22 to 38.96 μM correspondingly, showed great cytotoxic effect. Derivative **4a** and **5a** with IC_{50} = 63.63 and 59.63 μM respectively showed mild cytotoxicity.

Derivatives **4d**, **4e**, **4f**, **5e** and **5f** exhibited the greatest anticancer effect with IC_{50} = 16.59, 21.32, 17.71, 10.66 and 15.68 μM in that order against HCT-116. Moreover, derivatives **4b**, **4c**, **5a**, **5b**, **5c** and **5d** with IC_{50} ranging from 26.41 to 48.34 μM, showed potent cytotoxic effect. On the other hand derivative **3** with IC_{50} = 58.22 μM showed moderate cytotoxic activity.

Table 3 *In vitro* cytotoxic activities of the newly synthesized chemical compounds against HepG2, A549, MCF-7and HCT-116 cell lines VEGFR-2 and $EGFR^{T790M}$ kinases assays

	IC_{50}[a] (μM)					
Compound	HepG2	A549	MCF-7	HCT116	VEGFR-2	$EGFR^{T790M}$
4a	52.11 ± 5.2	51.00 ± 2.5	63.63 ± 3.8	58.22 ± 0.7	NT[b]	NT[b]
4b	35.40 ± 5.1	36.11 ± 1.9	36.89 ± 1.3	38.35 ± 3.9	NT[b]	NT[b]
4c	34.23 ± 5.1	38.32 ± 1.9	38.96 ± 1.3	42.52 ± 3.9	NT[b]	NT[b]
4d	13.47 ± 3.9	18.97 ± 3.9	22.73 ± 3.9	16.59 ± 3.9	0.255 ± 3.9	0.42 ± 3.9
4e	24.54 ± 3.9	33.97 ± 3.9	25.22 ± 3.9	21.32 ± 3.9	0.288 ± 3.9	0.52 ± 3.9
4f	10.24 ± 3.9	22.73 ± 3.9	22.29 ± 3.9	17.71 ± 3.9	0.095 ± 0.08	0.36 ± 3.9
4g	6.22 ± 3.9	12.92 ± 3.9	10.66 ± 3.9	11.17 ± 3.9	0.083 ± 3.9	0.23 ± 3.9
5a	52.11 ± 5.2	53.22 ± 2.5	59.63 ± 3.8	48.34 ± 0.7	NT[b]	NT[b]
5b	23.78 ± 3.9	36.22 ± 3.9	25.69 ± 3.9	28.22 ± 3.9	NT[b]	NT[b]
5c	24.12 ± 2.5	35.38 ± 1.9	28.61 ± 1.3	35.67 ± 3.9	NT[b]	NT[b]
5d	23.59 ± 3.9	29.66 ± 4.1	25.28 ± 4.5	26.41 ± 1.4	0.276 ± 3.9	0.52 ± 3.9
5e	23.76 ± 3.9	32.90 ± 3.9	14.54 ± 3.9	10.66 ± 3.9	0.263 ± 3.9	0.41 ± 3.9
5f	11.01 ± 3.9	13.02 ± 3.9	18.53 ± 3.9	15.68 ± 3.9	0.247 ± 3.9	0.35 ± 3.9
5g	3.86 ± 3.9	7.55 ± 3.9	10.65 ± 3.9	9.04 ± 3.9	0.080 ± 0.05	0.14 ± 3.9
Sorafenib	4.00 ± 0.33	4.04 ± 0.33	5.58 ± 0.55	5.05 ± 0.50	0.084 ± 0.04	NT[b]
Erlotinib	7.73 ± 0.67	5.49 ± 0.45	8.20 ± 0.34	13.91 ± 1.3	NT[b]	0.24 ± 0.22

[a] IC_{50} values are the mean ± S.D. of three separate experiments. [b] NT: compounds not tested.

2.4. *In vitro* VEGFR-2 kinase inhibitory assay

Additionally, as VEGFR-2 is mostly overexpressed in several malignancies such as HepG2, MCF-7 and HCT116, our most active cytotoxic compounds **4d**, **4e**, **4f**, **4g**, **5d**, **5e**, **5f** and **5g** were selected to assess their VEGFR-2 inhibitory effects as a result of applying an anti-phosphotyrosine antibody with the Alpha Screen system (PerkinElmer, USA).[43] The results were described as IC_{50} (50% inhibition concentration value) in Table 3. In this assessment, sorafenib was applied as a positive standard. The assessed derivatives demonstrated high to low inhibitory effect with IC_{50}vary between 0.080 to 0.288 μM. Derivatives **5g**, **4g** and **4f** were observed to be the highest effective derivatives that inhibited VEGFR-2 at IC_{50} = 0.080, 0.083 and 0.095 μM respectively. **5g** and **4g** showed more potent activities than that of sorafenib (IC_{50} = 0.084 μM). Moreover, compounds **4d**, **4e**, **5d**, **5e** and **5f** possessed moderate VEGFR-2 inhibitory effect with IC_{50} ranging from 0.247 to 0.288 μM.

2.5. $EGFR^{T790M}$ kinase inhibitory assay

Overexpression of EGFR is related to the increased poor prognosis, metastases and aggressiveness in various cancers such as A549 and HepG2 cell lines.[44] As a result, derivatives with effective cytotoxic activities **4d**, **4e**, **4f**, **4g**, **5d**, **5e**, **5f** and **5g** were additionally assessed to evaluate their inhibitory activities against mutant $EGFR^{T790M}$ kinase inhibitory activities. Homogeneous time resolved fluorescence (HTRF) assay was applied in this test.[45] Erlotinib was used as standard with IC_{50} = 0.24. Table 3 indicates a comparison of IC_{50} of the experienced derivatives.

Derivatives **5g** and **4g** could interfere with the $EGFR^{T790M}$ activity exhibiting stronger activities than elotinib with IC_{50} = 0.14 and 0.23 μM sequentially. Candidates **4d**, **4f**, **5e** and **5f** substantially inhibited $EGFR^{T790M}$ at IC_{50} ranging from 0.35 to 0.42 μM. Alternatively compounds **4e** and **5d** moderately inhibited $EGFR^{T790M}$ at the same IC_{50} = 0.52 μM.

2.6. Structure activity relationship (SAR)

The preliminary SAR study has focused on the effect of replacement of pyridine and the two 2-methoxyethoxy groups moieties of sorafenib and elotinib respectively by the heterocyclic furan and thiophene moieties. Also, it focused on the effect of replacement of the urea and amino linkers of sorafenib and elotinib respectively with acetamide linkers which interacting as H-bond acceptors through its carbonyl group and as H-bond donor through its NH atom. Moreover, the thiazolidine-2,4-dione was designed to replace the central aryl and quinazoline rings of the reference ligands sorafenib and elotinib respectively. On the other hand different substituents were introduced to the phenyl tail of our derivatives with different lipophilicity and electronic nature in order to study their effects on the anticancer activity. The data obtained revealed that, the tested structures displayed different levels of antitumor activity and possessed a distinctive pattern of selectivity toward the HepG2 cell lines. Generally, heterocyclic rings, the spacer, linker (HBA-HBD), lipophilicity and electronic nature of substituents exhibited an important role in anticancer activity. The furan ring as in compounds **5a–g** exhibited higher anticancer activities than the thiophene ones. Generally, the substituted phenyl tail as in compounds **4a–f** and **5a–f** showed higher anticancer activities than the unsubstituted **4g** and **5g** ones against the four HepG2, A549, MCF-7 and HCT116 cell lines.

From the structure of the synthesized derivatives and the data shown in Table 3 we can divide these tested compounds into two groups. The first group is compounds **4a–g** which containing thiophene heterocyclic ring; where derivative **4g** with electron withdrawing hydrophilic carboxylic group showed higher activities than **4f** with electron donating hydrophobic methoxy one against the four HepG2, A549, MCF-7 and HCT116 cell lines. Compound **4f** showed higher activities than **4d** with electron withdrawing hydrophobic bromo group against both HepG2 and MCF-7 but lower activities against both A549 and HCT116 cell lines. Furthermore, compound **4e** with hydrophobic electron donating methyl group showed higher activities than **4c** with electron withdrawing hydrophobic chloro group against the four cancer cell lines. In addition, derivative **4b** with chloro group exhibited higher activities than derivative **4c** with flouro one against A549, MCF-7 and HCT116 but lower activities against HepG2 cell lines. Finally, the unsubstituted derivative **4g** showed the least activities regarding the four cell lines.

The second group is compounds **5a–g** which containing furan heterocyclic ring; where derivative **5g** with electron withdrawing hydrophilic carboxylic group showed higher activities than **5f** with electron donating hydrophobic methoxy and **5d** with electron donating hydrophobic methyl ones against the four HepG2, A549, MCF-7 and HCT116 cell lines. Compound **5e** with electron donating hydrophobic isopropyl group showed higher activities than **5f** and **5d** against both MCF-7 and HCT116 but lower activities against both HepG2 and A549 cell lines respectively. Furthermore, compound **5b** with electron withdrawing hydrophobic chloro group exhibited higher activities than derivative **4c** with flouro one against HepG2, MCF-7 and HCT116 but lower activities against A549 cell lines. Finally, the unsubstituted derivative **5g** showed the least activities against the four cell lines.

2.7. ADMET; *in silico* studies profile

In silico report of the highly active derivatives **4g**, **5f** and **5g** was conducted for their physicochemical characters evaluation and the proposed ADMET profile. It was predicted using pkCSM descriptor algorithm procedures[46] and matched to rule of five described by Lipinski.[47] The good absorption properties were expected for the molecules that accomplish at least three rules: (i) hydrogen bond donors are not more than five; (ii) partition coefficient (log *P*) is not more than 5, (iii) molecular weight less than 500, (iv) hydrogen bond acceptors are not more than 10. In the current work, the standard anticancer agent sorafenib violates one rule while our new compounds **4g**, **5f** and **5g** and elotinib don't violate any one.

As a result of obtaining data (Table 4), we can assume that compound **5f** have very good GIT absorption in human (91.952)

Table 4 The highest effective compounds, sorafenib and elotinib; ADMET profile

Parameter	4g	5f	5g	Sorafenib	Erlotinib
Physicochemical properties					
Molecular weight	388.426	358.375	372.358	464.831	393.443
LogP	3.1213	2.9632	2.6528	5.5497	3.4051
Rotatable bonds	5	5	5	5	10
Acceptors	6	6	6	4	7
Donors	2	1	2	3	1
Surface area	155.861	147.173	151.015	185.111	169.532
Absorption					
Water solubility	−3.663	−4.262	−3.674	−4.822	−4.736
Caco2 permeability	1.012	1.088	0.839	0.689	1.431
Human intest. Absorption	56.765	91.952	55.558	89.043	94.58
Skin permeability	−2.735	−3.11	−2.735	−2.767	−2.741
Substrate for P-glycoprotein	+	+	+	+	—
Inhibitor of P-glycoprotein I	—	—	—	+	+
Inhibitor of P-glycoprotein II	—	—	—	+	+
Distribution					
VDss (human)	−1.173	−0.389	−1.294	−0.29	0.199
Human unbound fraction	0.213	0.224	0.352	0.065	0.059
Permeability throughout BBB	−1.447	−0.657	−1.496	−1.684	−0.745
Permeability to CNS	−2.413	−2.918	−3.009	−2.007	−3.216
Metabolism					
CYP2D6 substrate	—	—	—	—	—
CYP3A4 substrate	—	—	—	+	+
Inhibition of CYP3A4	—	—	—	+	+
Inhibition of CYP2D6	—	—	—	+	+
Inhibition of CYP2C9	—	—	—	+	+
Inhibition of CYP2C19	—	—	—	—	—
Inhibition of CYP1A2	—	+	—	+	+
Excretion					
Clearance	−0.199	0.054	−0.052	−0.219	0.702
Renal OCT2 substrate	—	—	—	—	—
Toxicity					
AMES toxicity	—	—	—	—	—
Human max. tolerated dose	0.199	−0.198	0.894	0.549	0.839
Inhibitor of hERG I	—	—	—	—	—
hERG II inhibitor	—	+	—	+	+
Acute toxic activity (LD_{50})	2.131	2.972	2.208	2.538	2.393
Chronic toxic activity (LOAEL)	0.914	0.627	0.3	1.198	1.37
Hepatotoxic effect	+	—	+	+	+
Skin sensitization	—	—	—	—	—
T. Pyriformis toxicity	0.287	0.951	0.286	0.383	0.309
Minnow toxic activity	0.395	0.794	1.524	0.189	−0.1

while compounds **4g** and **5g** have good absorption (56.765 and 55.558 respectively) which indicates easier to cross different biological membranes.[48] So, they may show a significant high bioavailability through GIT. Concerning CNS penetrability, our prepared compounds have the capability to reach CNS (CNS permeability values −2.413 to −3.009), lower than sorafenib (CNS permeability −2.007) but higher than elotinib (CNS permeability −3.216).

It well known that CYP3A4, the major drug metabolizing enzyme, could be inhibited by sorafenib and elotinib but **4g**, **5f** and **5g** could not. This is as well possibly for the superior lipophilicity of sorafenib and elotinib. Elimination was expected depending on the total clearance which is a considerable factor in deciding dose intervals. The data showed that elotinib confirmed higher clearance rates compared with sorafenib and our new compounds which demonstrated very low clearance values. Thus, elotinib, could be eliminated faster, and as a result supposed to have shorter dosing intervals. Unlike elotinib, the prepared compounds exhibited slowly clearance rate, which signifies longer duration of action and extended dosing intervals. Toxicityis the final ADMET profile studied factor. Like presented in Table 4, sorafenib, elotinib, and the novel compounds **4g** and **5g** shared the drawback of unwanted hepatotoxic actions but compound **5f** did not. Elotinib and **5g**

demonstrated the highest maximum tolerated dose. In contrast, sorafenib, **4g** and **5f** demonstrated the lowest maximum tolerated doses which involve the advantage of the broad therapeutic index of **5g** and elotinib respectively. Lastly, the oral chronic toxic doses of the novel compounds are lower than sorafenib and elotinib.

Finally, ADMET is in a good agreement with the experimental data obtained in many studies for thiazolidine-2,4-dions.[49]

3. Conclusion

In summary, fourteen new thiazolidine-2,4-dione-based derivatives have been designed, synthesized and evaluated for their anticancer activities against four human tumor cell lines HepG2, A549, MCF-7 and HCT-116 targeting both and VEGFR-2 and EGFR tyrosine kinases. The molecular design was performed to investigate the binding mode of the proposed compounds with VEGFR-2 and EGFR receptors. The data obtained from the docking studies were highly correlated with that obtained from the biological screening. All the tested compounds showed variable anticancer activities. HepG2 was the most sensitive cell line to the influence of the new derivatives. In particular, compounds **5g** and **4g** were observed to be the best effective compounds against HepG2 (IC_{50} = 3.86 and 6.22 μM), A549 (IC_{50} = 7.55 and 12.92 μM), MCF-7 (IC_{50} = 10.65 and 10.66 μM) and HCT116 (IC_{50} = 9.04 and 11.17 μM) tumor cell lines. Compound **5g** exhibited higher activities than sorafenib (IC_{50} = 4.00, 4.04, 5.58 and 5.05 μM) against HepG2 but lower activities *versus* A549, MCF-7 and HCT116 correspondingly. However, this compound demonstrated higher actions than Erlotinib (IC_{50} = 7.73, 5.49, 8.20 and 13.91 μM), against HepG2 and HCT116 but lower activities *versus* both A549 and MCF-7 correspondingly. However compound **4g** exhibited lower activities than sorafenib against the four cell lines, it also demonstrated higher actions than Erlotinib against HepG2 and HCT116 but lower activities *versus* both A549 and MCF-7 correspondingly. Derivatives **5g**, **4g** and **4f** were observed to be the highest effective derivatives that inhibited VEGFR-2 at IC_{50} = 0.080, 0.083 and 0.095 μM respectively. **5g** and **4g** showed more potent activities than that of sorafenib (IC_{50} = 0.084 μM). As well, compounds **5g** and **4g** could interfere with the $EGFR^{T790M}$ activity exhibiting stronger activities than Erlotinib with IC_{50} = 0.14 and 0.23 μM respectively. Moreover, ADMET profile was *in silico* calculated for the three most active compounds **4g**, **5f** and **5g** in comparing to sorafenib and Erlotinib as reference drugs. Our derivative **5f** have very good GIT absorption in human (91.952) while compounds **4g** and **5g** have good absorption (56.765 and 55.558 respectively) which indicates easier to cross different biological membranes. Unlike Erlotinib, the prepared compounds exhibited slowly clearance rate, which signifies longer duration of action and extended dosing intervals. Compound **5f** don't show the drawback of unwanted hepatotoxic actions. The obtained results showed that, our compounds specially **4g** and **5g** could be useful as a template for future design, optimization and investigation to produce more potent and selective dual VEGFR-2/$EGFR^{T790M}$ inhibitors with higher anticancer analogs.

4. Experimental

4.1. Chemistry

4.1.1. General. Starting and intermediate derivatives; thiazolidine-2,4-dione (**1**), 5-(thiophen-2-ylmethylene) thiazolidine-2,4-dione (**2**), 5-(furan-2-ylmethylene)thiazolidine-2,4-dione (**3**) and 2-chloro-*N*-(4-substitutedphenyl)acetamide were synthesized rendering to the reported procedures.[27]

All compounds were crystallized from ethanol and their NMR spectra were made in DMSO-d_6 solvent at 400 MHz for ^{1}HNMR and 100 MHz for ^{13}CNMR.

4.1.2. General procedure for the synthesis of the target compounds (4a–g). Equimolar quantities of 5-(thiophen-2-ylmethylene)thiazolidine-2,4-dione **2** (2.11 g, 0.01 mol) and the appropriate 2-chloro-*N*-(4-substitutedphenyl)acetamide derivative (0.01 mol) and potassium carbonate (1.5 g, 0.011 mol) in acetone (50 mL) were heated under reflux for 15 h. Then it was filtered while hot. The filtrate was allowed to obtain room temperature to get the target compounds **4a–g** respectively.

*4.1.2.1. 2-[2,4-Dioxo-5-(thiophen-2-ylmethylene)thiazolidin-3-yl]-N-phenylacetamide (**4a**).* Yield, 87%; mp 230–2 °C; $IR_{\nu max}$ (cm^{-1}): 3197 (NH), 3055 (CH aromatic), 2960 (CH aliphatic), 1714, 1667 (3C=O amide); ^{1}HNMR: 4.27 (s, 2H, CH_2), 6.72–6.79 (m, 1H, Ar–**H**, H-4 of phenyl), 7.02–7.07 (m, 1H, Ar–**H**, H-4 of thiophene), 7.19 (d, 1H, Ar–**H**, H-3 of thiophene), 7.54–7.58 (m, 2H, Ar–**H**, H-3 & H-5 of phenyl), 7.60 (s, 1H, C=C**H**), 7.61–7.82 (m, 2H, Ar–**H**, H-2 & H-6 of phenyl), 8.00–8.01 (d, 1H, Ar–**H**, H-5 of thiophene), 10.50 (s, 1H, NH, D_2O exchangeable); anal. calcd for $C_{16}H_{12}N_2O_3S_2$ (344.4): C, 55.80; H, 3.51; N, 8.13. Found: C, 55.90; H, 3.58; N, 8.09.

*4.1.2.2. N-(4-Chlorophenyl)-2-[2,4-dioxo-5-(thiophen-2-ylmethylene)thiazolidin-3-yl]acetamide (**4b**).* Yield, 84%; mp 240–2 °C; $IR_{\nu max}$ (cm^{-1}): 3250 (NH), 3100 (CH aromatic), 2917 (CH aliphatic), 1704, 1649 (3C=O amide); ^{1}HNMR: 4.10 (s, 1H, CH_2), 4.52 (s, 1H, CH_2), 7.26–7.34 (m, 2H, Ar–**H**, H-2 & H-6 of phenyl), 7.37–7.40 (m, 1H, Ar–**H**, H-4 of thiophene), 7.53–7.60 (m, 2H, Ar–**H**, H-3 & H-5 of phenyl), 7.77 (s, 1H, C=C**H**), 7.99 (d, 1H, Ar–**H**, H-3 of thiophene), 8.09–8.28 (d, 1H, Ar–**H**, H-5 of thiophene), 10.58 (s, 1H, NH, D_2O exchangeable); LC-MS ESI spectrometry in the negative ion mode: the mass spectrum of compound **4b** showed M + 2 molecular ion peak at 379.0852 and base peak at 377.1044; anal. calcd for $C_{16}H_{11}ClN_2O_3S_2$ (378.8): C, 50.73; H, 2.93; N, 7.39. Found: C, 50.76; H, 2.95; N, 7.44.

*4.1.2.3. 2-[2,4-Dioxo-5-(thiophen-2-ylmethylene)thiazolidin-3-yl]-N-(4-fluorophenyl)acetamide (**4c**).* Yield, 73%; mp 245–7 °C; $IR_{\nu max}$ (cm^{-1}): 3288 (NH), 3050 (CH aromatic), 2950 (CH aliphatic), 1782, 1712, 1650 (3C=O amide); ^{1}HNMR: 4.50 (s, 2H, CH_2), 7.15–7.31 (m, 2H, Ar–**H**, H-2 & H-6 of phenyl), 7.38–7.42 (m, 1H, Ar–**H**, H-4 of thiophene), 7.56–7.59 (m, 2H, Ar–**H**, H-3 & H-5 of phenyl), 7.76 (s, 1H, C=C**H**), 7.77 (d, 1H, Ar–**H**, H-3 of thiophene), 8.27 (d, 1H, Ar–**H**, H-5 of thiophene), 10.44 (s, 1H, NH, D_2O exchangeable); ^{13}CNMR: 44.53, 115.84, 116.06, 118.61, 121.47, 121.55, 125.42, 127.44, 129.29, 134.31, 135.19, 137.41, 164.25, 165.52, 167.07, 171.49; LC-MS ESI spectrometry in the

positive ion mode: the mass spectrum of compound **4c** showed M molecular ion peak at 362.4517 and base peak at 318.4247; LC-MS ESI spectrometry in the negative ion mode: M − 1 molecular ion peak at 361.1305 which also was the base peak. It showed M molecular ion peak at 362.1415 and M + 1 molecular ion peak at 363.1041; anal. calcd for $C_{16}H_{11}FN_2O_3S_2$ (362.4): C, 53.03; H, 3.06; N, 7.73; found: C, 52.98; H, 3.04; N, 7.66.

*4.1.2.4. N-(4-Bromophenyl)-2-[2,4-dioxo-5-(thiophen-2-ylmethylene)thiazolidin-3-yl]acetamide (**4d**).* Yield, 70%; mp 238–9 °C; $IR_{\nu max}$ (cm^{-1}): 3150 (NH), 3050 (CH aromatic), 2950 (CH aliphatic), 1747, 1669 (3C=O amide); ^{1}HNMR: 4.53 (s, 2H, CH_2), 7.14–7.32 (m, 1H, Ar–**H**, H-4 of thiophene), 7.34–7.44 (m, 3H, Ar–**H**, H-2 & H-6 of phenyl & H-3 of thiophene), 7.76–7.77 (m, 2H, Ar–**H**, H-3 & H-5 of phenyl), 8.07 (s, 1H, C=C**H**), 8.28 (d, 1H, Ar–**H**, H-5 of thiophene), 10.60 (s, 1H, NH, D_2O exchangeable); ^{13}CNMR: 44.61, 118.09, 118.54, 119.19, 124.00, 127.51, 129.62, 131.11, 133.67, 134.33, 135.89, 137.38, 140.18, 164.76, 165.49, 166.95; anal. calcd for $C_{16}H_{11}BrN_2O_3S_2$ (423.3): C, 45.40; H, 2.62; N, 6.62; found: C, 45.40; H, 2.55; N, 6.60.

*4.1.2.5. 2-[2,4-Dioxo-5-(thiophen-2-ylmethylene)thiazolidin-3-yl]-N-(p-tolyl)acetamide (**4e**).* Yield, 70%; mp 278–9 °C; $IR_{\nu max}$ (cm^{-1}): 3368 (NH), 3050 (CH aromatic), 2950 (CH aliphatic), 1697 (3C=O amide); ^{1}HNMR: 2.25 (s, 3H, CH_3), 4.49 (s, 2H, CH_2), 7.12–7.14 (m, 2H,Ar–**H**, H-3 & H-5 of phenyl), 7.32–7.34 (m, 1H, Ar–**H**, H-4 of thiophene), 7.42–7.44 (m, 2H, Ar–**H**, H-2 & H-6 of phenyl), 7.76 (d, 1H, Ar–**H**, H-3 of thiophene), 8.07 (d, 1H, Ar–**H**, H-5 of thiophene), 8.27 (s, 1H, C=C**H**), 10.28 (s, 1H, NH, D_2O exchangeable); ^{13}CNMR: 20.66, 56.67, 83.08, 100.64, 106.69, 113.92, 119.97 (2), 130.15 (3), 133.69, 135.91, 167.49, 183.13, 203.35, 208.81; anal. calcd for $C_{17}H_{14}N_2O_3S_2$ (358.4): C, 56.97; H, 3.94; N, 7.82; found: C, 57.06; H, 4.05; N, 7.77.

*4.1.2.6. 2-[2,4-Dioxo-5-(thiophen-2-ylmethylene)thiazolidin-3-yl]-N-(4-methoxyphenyl)acetamide (**4f**).* Yield, 73%; mp 284–6 °C; $IR_{\nu max}$ (cm^{-1}): 3250 (NH), 3068 (CH aromatic), 2933 (CH aliphatic), 1779, 1714 (4C=O amide); ^{1}HNMR: 3.80 (s, 3H, CH_3), 4.08 (s, 2H, CH_2), 6.99–7.02 (m, 2H,Ar–**H**, H-3 & H-5 of phenyl), 7.11–7.13 (m, 2H, Ar–**H**, H-2 & H-6 of phenyl), 7.23–7.27 (m, 1H, Ar–**H**, H-4 of thiophene), 7.74 (s, 1H, C=C**H**), 7.75–7.97 (d, 1H, Ar–**H**, H-3 of thiophene), 7.98–8.27 (d, 1H, Ar–**H**, H-5 of thiophene), 10.25 (s, 1H, NH, D_2O exchangeable); ^{13}CNMR: 31.09, 55.78, 114.50, 114.65, 118.56, 121.36, 128.41, 128.66 (2), 130.09, 132.26, 133.16, 136.18, 138.09, 159.27, 164.18, 168.60; MS (*m*/*z*): 375 (M^+ + 1, 6.54%), 374 (M^+, 47.45%), 331 (100%, base beak), 274 (7.33%), 95 (13.49%); anal. calcd for $C_{17}H_{14}N_2O_4S_2$ (374.4): C, 54.53; H, 3.77; N, 7.48; found: C, 54.44; H, 3.75; N, 7.55.

*4.1.2.7. 4-{2-[2,4-Dioxo-5-(thiophen-2-ylmethylene) thiazolidin-3-yl]acetamido}benzoic acid (**4g**).* Yield, 80%; mp 260–2 °C; $IR_{\nu max}$ (cm^{-1}): 3450 (OH), 3114 (NH), 3025 (CH aromatic), 2965 (CH aliphatic), 1729, 1672 (3C=O amide); ^{1}HNMR: 4.26 (s, 1H, CH_2), 4.54 (s, 1H, CH_2), 7.14–7.42 (m, 4H, Ar–**H** of phenyl), 7.52–7.61 (m, 2H, Ar–**H**, H-3 & H-4 of thiophene), 7.62 (d, 1H, Ar–**H**, H-5 of thiophene), 8.30 (s, 1H, C=C**H**), 10.50 (s, 1H, NH, D_2O exchangeable), 10.65 (s, 1H, OH, D_2O exchangeable); MS (*m*/*z*): 388 (M^+, 59.76%), 326 (94.26%), 302 (92.19%), 225 (91.25%), 84 (98.76%), 43 (100%, base beak); LC-MS ESI spectrometry in the positive ion mode: M molecular ion peak at 388.2247 which also was the base peak. It showed M + 2 and M + 3 molecular ion peaks at 390.2077 and 391.2493 respectively; anal. calcd for $C_{17}H_{12}N_2O_5S_2$ (388.4): C, 52.57; H, 3.11; N, 7.21; found: C, 52.51; H, 3.15; N, 7.15.

4.1.3. General procedure for the synthesis of the target compounds (5a–g). Equimolar quantities of 5-(furan-2-ylmethylene)thiazolidine-2,4-dione **3** (1.95 g, 0.01 mol) and the appropriate 2-chloro-*N*-(4-substitutedphenyl)acetamide derivative (0.01 mol) and potassium carbonate (1.5 g, 0.011 mol) in acetone (50 mL) were heated under reflux for 15 h. Then it was filtered while hot. The filtrate was allowed to obtain room temperature to get the target compounds **5a–g** respectively.

*4.1.3.1. 2-[5-(Furan-2-ylmethylene)-2,4-dioxothiazolidin-3-yl]-N-phenylacetamide (**5a**).* Yield, 77%; mp 240–2 °C; $IR_{\nu max}$ (cm^{-1}): 3212 (NH), 3050 (CH aromatic), 2950 (CH aliphatic), 1713, 1667 (3C=O amide); ^{1}HNMR: 4.47 (s, 2H, CH_2), 7.04–7.10 (m, 2H, Ar–**H**, H-4 of furan & H-4 of phenyl), 7.27–7.31 (m, 2H, Ar–**H**, H-3 & H-5 of phenyl), 7.35–7.41 (m, 2H, Ar–**H**, H-2 & H-6 of phenyl), 7.44–7.54 (m, 2H, Ar–**H**, H-3 of furan & C=C**H**), 7.56–7.71 (m, 1H, Ar–**H**, H-5 of furan), 10.38 (s, 1H, NH, D_2O exchangeable); anal. calcd for $C_{16}H_{12}N_2O_4S$ (328.3): C, 58.53; H, 3.68; N, 8.53. Found: C, 58.46; H, 3.73; N, 8.55.

*4.1.3.2. N-(4-Chlorophenyl)-2-[5-(furan-2-ylmethylene)-2,4-dioxothiazolidin-3-yl]acetamide (**5b**).* Yield, 75%; mp 247–9 °C; $IR_{\nu max}$ (cm^{-1}): 3114 (NH), 3025 (CH aromatic), 2965 (CH aliphatic), 1729, 1672 (3C=O amide); ^{1}HNMR: 4.56 (s, 1H, CH_2), 4.65 (s, 1H, CH_2), 7.25–7.28 (m, 2H, Ar–**H**, H-3 & H-5 of phenyl), 7.62–7.63 (m, 2H, Ar–**H**, H-2 & H-6 of phenyl), 7.71–7.73 (m, 1H, Ar–**H**, H-4 of furan), 7.90 (s, 1H, C=C**H**), 7.92–8.00 (m, 2H, Ar–**H**, H-3 & H-5 of furan), 10.73 (s, 1H, NH, D_2O exchangeable); anal. calcd for $C_{16}H_{11}ClN_2O_4S$ (362.8): C, 52.97; H, 3.06; N, 7.72. Found: C, 53.07; H, 3.12; N, 7.74.

*4.1.3.3. N-(4-Fluorophenyl)-2-[5-(furan-2-ylmethylene)-2,4-dioxothiazolidin-3-yl]acetamide (**5c**).* Yield, 72%; mp 242–4 °C; $IR_{\nu max}$ (cm^{-1}): 3160 (NH), 3041 (CH aromatic), 2950 (CH aliphatic), 1665 (3C=O amide); ^{1}HNMR: 4.49 (s, 2H, CH_2), 6.76–6.78 (m, 1H, Ar–**H**, H-4 of furan), 7.13–7.18 (m, 3H, Ar–**H**, H-3 & H-5 of phenyl & H-3 of furan), 7.57–7.60 (m, 2H, Ar–**H**, H-2 & H-6 of phenyl), 7.81 (s, 1H, C=C**H**), 8.08 (d, 1H, Ar–**H**, H-5 of furan), 10.50 (s, 1H, NH, D_2O exchangeable); LC-MS ESI spectrometry in the negative ion mode: M − 1 molecular ion peak at 345.1374 which also was the base peak; anal. calcd for $C_{16}H_{11}FN_2O_4S$ (346.3): C, 55.49; H, 3.20; N, 8.09. Found: C, 55.55; H, 3.24; N, 8.25.

*4.1.3.4. 2-[5-(Furan-2-ylmethylene)-2,4-dioxothiazolidin-3-yl]-N-(p-tolyl)acetamide (**5d**).* Yield, 77%; mp 247–9 °C; $IR_{\nu max}$ (cm^{-1}): 3138 (NH), 3092 (CH aromatic), 2956 (CH aliphatic), 1668 (3C=O amide); ^{1}HNMR: 2.24 (s, 3H, CH_3), 4.23 (s, 2H, CH_2), 6.88–6.95 (m, 1H, Ar–**H**, H-4 of furan), 7.00–7.14 (m, 2H, Ar–**H**, H-3 & H-5 of phenyl), 7.25–7.41 (m, 2H, Ar–**H**, H-2 & H-6 of phenyl), 7.43–7.69 (m, 2H, H-3 of furan & C=C**H**), 7.70 (d, 1H, Ar–**H**, H-5 of furan), 10.23 (s, 1H, NH, D_2O exchangeable); ^{13}CNMR: 20.80, 61.89, 120.02, 120.12, 123.52, 124.94, 128.17, 129.42, 129.57, 130.30, 132.95, 133.85, 135.85, 144.11, 165.14, 167.19, 168.24; MS (*m*/*z*): 344 (M^+ + 2, 3.97%), 342 (M^+, 73.12%), 273 (81.03%), 271 (82.51%), 115 (100%, base beak); anal. calcd

for $C_{17}H_{14}N_2O_4S$ (342.4): C, 59.64; H, 4.12; N, 8.18. Found: C, 59.75; H, 4.15; N, 8.20.

*4.1.3.5. 2-[5-(Furan-2-ylmethylene)-2,4-dioxothiazolidin-3-yl]-N-(4-isopropylphenyl)acetamide (**5e**).* Yield, 80%; mp 287–9 °C; $IR_{\nu max}$ (cm^{-1}): 3320 (NH), 3100 (CH aromatic), 2958 (CH aliphatic), 1669 (3C=O amide); ^{1}HNMR: 1.17 (d, 6H, $2CH_3$), 2.83–2.87 (m, 1H, CH), 4.44 (s, 2H, CH_2), 7.01–7.08 (m, 1H, Ar–**H**, H-4 of furan), 7.18–7.20 (m, 2H, Ar–**H**, H-3 & H-5 of phenyl), 7.36–7.47 (m, 3H, Ar–**H**, H-2 & H-6 of phenyl & C=C**H**), 7.67–7.71 (m, 2H, Ar–**H**, H-3 & H-5 of furan), 10.30 (s, 1H, NH, D_2O exchangeable); ^{13}CNMR: 24.30 (2), 33.27, 44.23, 119.78 (2), 122.41, 123.44, 127.09 (2), 128.40, 129.48, 130.60, 134.50, 135.79, 144.77, 145.08, 165.34, 167.64; anal. calcd for $C_{19}H_{18}N_2O_4S$ (370.4): C, 61.61; H, 4.90; N, 7.56. Found: C, 61.55; H, 4.95; N, 7.50.

*4.1.3.6. 2-[5-(Furan-2-ylmethylene)-2,4-dioxothiazolidin-3-yl]-N-(4-methoxyphenyl)acetamide (**5f**).* Yield, 76%; mp 283–5 °C; $IR_{\nu max}$ (cm^{-1}): 3300 (NH), 3050 (CH aromatic), 2950 (CH aliphatic), 1670 (3C=O amide); ^{1}HNMR: 3.72 (s, 3H, OCH_3), 4.46 (s, 2H, CH_2), 6.78–6.80 (m, 1H, Ar–**H**, H-4 of furan), 6.88 (d, 2H, Ar–**H**, H-3 & H-5 of phenyl), 7.18–7.25 (m, 1H, Ar–**H**, H-3 of furan), 7.25 (d, 2H, Ar–**H**, H-2 & H-6 of phenyl), 7.82 (s. 1H, C=C**H**), 8.10 (d, 1H, Ar–**H**, H-5 of furan), 10.30 (s, 1H, NH, D_2O exchangeable); ^{13}CNMR: 44.21, 55.63, 114.19, 114.45, 118.05, 120.07, 120.42, 121.24, 128.60, 131.92, 148.43, 149.60, 155.97, 163.82, 165.60, 168.39, 183.79; MS (*m*/*z*): 359 (M^+ + 1, 5.97%), 358 (M^+, 25.42%), 236 (12.33%), 208 (46.57%), 124 (90.17%), 123 (100%, base beak); anal. calcd for $C_{17}H_{14}N_2O_5S$ (358.4): C, 56.98; H, 3.94; N, 7.82. Found: C, 57.11; H, 4.06; N, 7.76.

*4.1.3.7. 4-{2-[5-(Furan-2-ylmethylene)-2,4-dioxothiazolidin-3-yl]acetamido}benzoic acid (**5g**).* Yield, 83%; mp 275–7 °C; $IR_{\nu max}$ (cm^{-1}): 3375 (OH), 3200 (NH), 3050 (CH aromatic), 2950 (CH aliphatic), 1730, 1655 (4C=O amide); ^{1}HNMR: 4.74 (s, 2H, CH_2), 7.31–7.42 (m, 2H, Ar–**H**, H-4 of furan & C=C**H**), 7.60–7.62 (m, 2H, Ar–**H**, H-3 & H-5 of furan), 7.64–7.74 (m, 2H, Ar–**H**, H-2 & H-6 of phenyl), 7.75–7.92 (m, 2H, Ar–**H**, H-3 & H-5 of phenyl), 10.02 (s, 1H, OH, D_2O exchangeable), 10.92 (s, 1H, NH, D_2O exchangeable); anal. calcd for $C_{17}H_{12}N_2O_6S$ (372.4): C, 54.84; H, 3.25; N, 7.52. Found: C, 55.06; H, 3.35; N, 7.60.

Author contributions

K. El-Adl, Riham F. George and Walaa R. Mahmoud were responsible for the conception and rational design of the work. K. El-Adl and Nada A. A. M. Aziz were responsible for the data collection and synthesis of the new compounds. K. El-Adl performed the molecular docking study. Riham F. George, Walaa R. Mahmoud and K. El-Adl were responsible for spectral data analysis. Walaa R. Mahmoud and Nada A. A. M. Aziz conducted the cytotoxicity assay. Nada A. A. M. Aziz and K. El-Adl conducted the *in silico* pharmacokinetic study. All authors discussed the results and contributed to the writing and revision of the original manuscript.

Conflicts of interest

There are no conflicts to declare.

Acknowledgements

The authors extend their appreciation and thanking to Dr Mohamed Ragab, Pharmacology & Toxicology Department, Faculty of Pharmacy, Al-Azhar University, Cairo, Egypt for helping in the pharmacological part.

References

1 D. Panigrahy, *et al.*, PPARγ ligands inhibit primary tumor growth and metastasis by inhibiting angiogenesis, *The Journal of clinical investigation*, 2002, **110**(7), 923–932.
2 H. Joshi, T. Pal and C. Ramaa, A new dawn for the use of thiazolidinediones in cancer therapy, *Expert Opin. Invest. Drugs*, 2014, **23**(4), 501–510.
3 U. Bhanushali, *et al.*, 5-Benzylidene-2, 4-thiazolidenedione derivatives: Design, synthesis and evaluation as inhibitors of angiogenesis targeting VEGR-2, *Bioorg. Chem.*, 2016, **67**, 139–147.
4 E. S. Ch'ng, H. Jaafar and S. E. Tuan Sharif, Breast tumor angiogenesis and tumor-associated macrophages: histopathologist's perspective, *Pathol. Res. Int.*, 2011, **2011**, 1–15.
5 X. Le, M. Nilsson, J. Goldman, M. Reck, K. Nakagawa, T. Kato, L. P. Ares, B. Frimodt-Moller, K. Wolff, C. Visseren-Grul, J. V. Heymach and E. B. Garon, Dual EGFR-VEGF Pathway Inhibition: A Promising Strategy for Patients With EGFR-Mutant NSCLC, *J. Thorac. Oncol.*, 2021, **16**(2), 205–215, DOI: 10.1016/j.jtho.2020.10.006.
6 A. Midha, S. Dearden and R. McCormack, EGFR mutation incidencein non-small-cell lung cancer of adenocarcinoma histology: a systematic review and global map by ethnicity (mutMapII), *Am. J. Cancer Res.*, 2015, **5**, 2892–2911.
7 P. A. Jänne, J. C. Yang, D. W. Kim, *et al.*, AZD9291 in EGFR inhibitor-resistant non-small-cell lung cancer, *N. Engl. J. Med.*, 2015, **372**, 1689–1699.
8 J. J. Lin, S. Cardarella, C. A. Lydon, *et al.*, Five-year survival in EGFR-mutant metastatic lung adenocarcinoma treatedwith EGFR-TKIs, *J. Thorac. Oncol.*, 2016, **11**, 556–565.
9 A. K. Larsen, D. Ouaret, K. El Ouadrani and A. Petitprez, Targeting EGFR and VEGF(R) pathway cross-talk in tumor survivaland angiogenesis, *Pharmacol. Ther.*, 2011, **131**, 80–90.
10 P. M. Hoff and K. K. Machado, Role of angiogenesis in the pathogenesis of cancer, *Cancer Treat. Rev.*, 2012, **38**(7), 825–833.
11 Z. K. Otrock, J. A. Makarem and A. I. Shamseddine, Vascular endothelial growth factor family of ligands and receptors, *Blood Cells, Mol., Dis.*, 2007, **38**(3), 258–268.
12 E. Gershtein, *et al.*, Vascular endothelial growth factor and its type 2 receptor in hepatocellular carcinoma, *Bull. Exp. Biol. Med.*, 2010, **149**(6), 749.
13 D. K. Shah, *et al.*, Thiazolidinediones decrease vascular endothelial growth factor (VEGF) production by human luteinized granulosa cells in vitro, *Fertil. Steril.*, 2010, **93**(6), 2042–2047.

14 S. Takahashi, Vascular endothelial growth factor (VEGF), VEGF receptors and their inhibitors for antiangiogenic tumor therapy, *Biol. Pharm. Bull.*, 2011, **34**(12), 1785–1788.

15 P. Wu, T. E. Nielsen and M. H. Clausen, FDA-approved small-molecule kinase inhibitors, *Trends Pharmacol. Sci.*, 2015, **36**(7), 422–439.

16 T. Francis, S. R. Dixit and B. R. P. Kumar, Discovery of Rhodanine and Thiazolidinediones as Novel Scaffolds for EGFR Inhibition: Design, Synthesis, Analysis and CoMSIA Studies, *Polycyclic Aromat. Compd.*, 2020, 1–17, DOI: **10.1080/10406638.2020.1836004**.

17 Y. Chen, J. Wu, A. Wang, Z. Qi, T. Jiang, C. Chen, F. Zou, C. Hu, W. Wang and H. Wu, Discovery of N-(5-((5-chloro-4-((2-(isopropylsulfonyl) phenyl) amino) pyrimidin-2-yl) amino)-4-methoxy-2-(4-methyl-1, 4-diazepan-1-yl) phenyl) acrylamide (CHMFL-ALK/EGFR-050) as a potent ALK/EGFR dual kinase inhibitor capable of overcoming a variety of ALK/EGFR associated drug resistant mutants in NSCLC, *Eur. J. Med. Chem.*, 2017, **139**, 674–697.

18 J. Chang, H. Ren, M. Zhao, Y. Chong, W. Zhao, Y. He, Y. Zhao, H. Zhang and C. Qi, Development of a series of novel 4-anlinoquinazoline derivatives possessing quinazoline skeleton: Design, synthesis, EGFR kinase inhibitory efficacy, and evaluation of anticancer activities in vitro, *Eur. J. Med. Chem.*, 2017, **138**, 669–688.

19 Y. A. Elshaier, M. A. Shaaban, M. K. A. El Hamid, M. H. Abdelrahman, M. A. Abou-Salim, S. M. Elgazwi and F. Halaweish, Design and synthesis of pyrazolo [3, 4-d] pyrimidines: Nitric oxide releasing compounds targeting hepatocellular carcinoma, *Biorg. Med. Chem.*, 2017, **25**(12), 2956–2970.

20 H.-Q. Zhang, F.-H. Gong, J.-Q. Ye, C. Zhang, X.-H. Yue, C.-G. Li, Y.-G. Xu and L.-P. Sun, Design and discovery of 4-anilinoquinazoline-urea derivatives as dual TK inhibitors of EGFR and VEGFR-2, *Eur. J. Med. Chem.*, 2017, **125**, 245–254.

21 M. L. D. C. Barbosa, L. M. Lima, R. Tesch, C. M. R. SantAnna, F. Totzke, M. H. G. Kubbutat, C. Schachtele, S. A. Laufer and E. J. Barreiro, Novel 2-chloro-4-anilino-quinazoline derivatives as EGFR and VEGFR-2 dual inhibitors, *Eur. J. Med. Chem.*, 2014, **71**, 1–14.

22 A. Garofalo, L. Goossens, A. Lemoine, S. Ravez, P. Six, M. Howsam, A. Farce and P. Depreux, [4-(6,7-Disubstituted quinazolin-4-ylamino)phenyl] carbamic acid esters: a novel series of dual EGFR/VEGFR-2 tyrosine kinase inhibitors, *Med. Chem. Commun*, 2011, **2**, 65–72.

23 K. El-Adl, A. -H. Abdel-Rahman, A. M. Omar, M. Alswah and N. M. Saleh, *Arch. Pharm.*, 2021, e2100237, DOI: **10.1002/ardp.202100237**.

24 V. Gandin, A. Ferrarese, M. Dalla Via, C. Marzano, A. Chilin and G. Marzaro, Targeting kinases with anilinopyrimidines: discovery of N-phenyl-N'-[4-(pyrimidin-4-ylamino) phenyl] urea derivatives as selective inhibitors of class III receptor tyrosine kinase subfamily, *Sci. Rep.*, 2015, **5**, 16750.

25 K. El-Adl, H. Sakr, M. Nasser and F. M. A. Shoman, *Arch. Pharm.*, 2020, e2000079, DOI: **10.1002/ardp.202000079**.

26 K. El-Adl, A. A. El-Helby, H. Sakr and S. S. A. El-Hddad, *Arch. Pharm.*, 2020, e2000068, DOI: **10.1002/ardp.202000068**.

27 K. El-Adl, A. A. El-Helby, H. Sakr, I. H. Eissa, S. S. A. El-Hddad and F. M. A. Shoman, *Bioorg. Chem.*, 2020, **102**, 104059, DOI: **10.1016/j.bioorg.2020.104059**.

28 A. M. Sayed, F. A. Taher, M. R. K. Abdel-Samad, M. S. A. El-Gaby, K. El-Adl and N. M. Saleh, *Bioorg. Chem.*, 2021, **108**, 104669, DOI: **10.1016/j.bioorg.2021.104669**, Epub 2021 Jan 21. PMID: 33515863, .

29 N. M. Saleh, M. S. A. El-Gaby, K. El-Adl and N. E. A. Abd El-Sattar, *Bioorg. Chem.*, 2020, **104**, 104350, DOI: **10.1016/j.bioorg.2020.104350**.

30 K. El-Adl, A. A. El-Helby, H. Sakr and A. Elwan, *Bioorg. Chem.*, 2020, **105**, 104399, DOI: **10.1016/j.bioorg.2020.104399**.

31 K. El-Adl, A. A. El-Helby, H. Sakr and A. Elwan, *New J. Chem.*, 2021, **45**, 881, DOI: **10.1039/D0NJ02990D**.

32 N. E. A. Abd El-Sattar, K. El-Adl, M. A. El-Hashash, S. A. Salama and M. M. Elhady, *Bioorg. Chem.*, 2021, **22**(115), 105186, DOI: **10.1016/j.bioorg.2021.105186**. Epub ahead of print. PMID: 34314914, .

33 Q.-Q. Xie, *et al.*, Pharmacophore modeling studies of type I and type II kinase inhibitors of Tie2, *J. Mol. Graphics Modell.*, 2009, **27**(6), 751–758.

34 K. Lee, *et al.*, Pharmacophore modeling and virtual screening studies for new VEGFR-2 kinase inhibitors, *Eur. J. Med. Chem.*, 2010, **45**(11), 5420–5427.

35 V. A. Machado, *et al.*, Synthesis, antiangiogenesis evaluation and molecular docking studies of 1-aryl-3-[(thieno [3, 2-b] pyridin-7-ylthio) phenyl] ureas: Discovery of a new substitution pattern for type II VEGFR-2 Tyr kinase inhibitors, *Bioorg. Med. Chem.*, 2015, **23**(19), 6497–6509.

36 Z. Wang, *et al.*, Dietary compound isoliquiritigenin inhibits breast cancer neoangiogenesis via VEGF/VEGFR-2 signaling pathway, *PLoS One*, 2013, **8**(7), e68566.

37 J. Dietrich, C. Hulme and L. H. Hurley, The design, synthesis, and evaluation of 8 hybrid DFG-out allosteric kinase inhibitors: A structural analysis of the binding interactions of Gleevec®, Nexavar®, and BIRB-796, *Bioorg. Med. Chem.*, 2010, **18**(15), 5738–5748.

38 Z. Zhao, H. Wu, L. Wang, Y. Liu, S. Knapp, Q. Liu and N. S. Gray, Exploration of type II binding mode: a privileged approach for kinase inhibitor focused drug discovery?, *ACS Chem. Biol.*, 2014, **9**(6), 1230–1241.

39 S. A. Elmetwally, K. F. Saied, I. H. Eissa and E. B. Elkaeed, Design, synthesis and anticancer evaluation of thieno[2,3-d]pyrimidine derivatives as dual EGFR/HER2 inhibitors and apoptosis inducers, *Bioorg. Chem.*, 2019, **88**, 102944, DOI: **10.1016/j.bioorg.2019.102944**.

40 F. Khedr, M.-K. Ibrahim, I. H. Eissa, H. S. Abulkhair and K. El-Adl, *Arch. Pharm.*, 2021, e2100201, DOI: **10.1002/ardp.202100201**.

41 T. Mosmann, Rapid colorimetric assay for cellular growth and survival: application to proliferation and cytotoxicity assays, *J. Immunol. Methods*, 1983, **65**(1–2), 55–63.

42 F. M. Freimoser, *et al.*, The MTT [3-(4, 5-dimethylthiazol-2-yl)-2, 5-diphenyltetrazolium bromide] assay is a fast and reliable method for colorimetric determination of fungal

cell densities, *Appl. Environ. Microbiol.*, 1999, **65**(8), 3727–3729.

43 S. M. Abou-Seri, *et al.*, 1-Piperazinylphthalazines as potential VEGFR-2 inhibitors and anticancer agents: synthesis and in vitro biological evaluation, *Eur. J. Med. Chem.*, 2016, **107**, 165–179.

44 C. Deng, J. Xiong, X. Gu, X. Chen, S. Wu, Z. Wang, D. Wang, J. Tu and J. Xie, Novel recombinant immunotoxin of EGFR specific nanobody fused with cucurmosin, construction and antitumor efficiency in vitro, *Oncotarget*, 2017, **8**(24), 38568–38580.

45 Y. Jia, C. M. Quinn, A. I. Gagnon and R. Talanian, Homogeneous time-resolved fluorescence and its applications for kinase assays in drug discovery, *Anal. Biochem.*, 2006, **356**(2), 273–281.

46 C. A. Lipinski, F. Lombardo, B. W. Dominy and P. J. Feeney, *Adv. Drug Deliv. Rev.*, 1997, **23**, 3, DOI: **10.1016/S0169-409X(96)00423-1**.

47 D. E. V. Pires, T. L. Blundell and D. B. Ascher, *J. Med. Chem.*, 2015, **58**, 4066, DOI: **10.1021/acs.jmedchem.5b00104**.

48 A. Beig, R. Agbaria and A. Dahan, *PLoS One*, 2013, **8**, e68237, DOI: **10.1371/journal.pone.0068237**.

49 G. Marc, A. Stana, A. Pîrnău, L. Vlase, D. C. Vodnar, M. Duma, B. Tiperciuc and O. Oniga, 3,5-Disubstituted Thiazolidine-2,4-Diones: Design, Microwave-Assisted Synthesis, Antifungal Activity, and ADMET Screening, *SLAS Discovery*, 2018, **23**(8), 807–814, DOI: **10.1177/2472555218759035**.